Defense Special Weapons Agency
Alexandria, VA 22310-3398

DSWA-TR-96-46

DAA-Based Computational Boundaries for Ground-Shock Analysis
Volume 1–DAA Formulation and Canonical Comparisons

Brett A. Lewis
Thomas L. Geers
University of Colorado
Mechanical Engineering Dept
Campus Box 19
Boulder CO 80903

December 1997

Technical Report

CONTRACT No. DNA 001-92-C-0038

Approved for public release;
distribution is unlimited.

DESTRUCTION NOTICE:

Destroy this report when it is no longer needed.
Do not return to sender.

PLEASE NOTIFY THE DEFENSE SPECIAL WEAPONS AGENCY, ATTN: CSTI, 6801TELEGRAPH ROAD, ALEXANDRIA, VA 22310-3398, IF YOUR ADDRESS IS INCORRECT, IF YOU WISH IT DELETED FROM THE DISTRIBUTION LIST, OR IF THE ADDRESSEE IS NO LONGER EMPLOYED BY YOUR ORGANIZATION.

DISTRIBUTION LIST UPDATE

This mailer is provided to enable DSWA to maintain current distribution lists for reports. (We would appreciate your providing the requested information.)

NOTE:
Please return the mailing label from the document so that any additions, changes, corrections or deletions can be made easily. For distribution cancellation or more information call DSWA/IMAS (703) 325-1036.

☐ Add the individual listed to your distribution list.

☐ Delete the cited organization/individual.

☐ Change of address.

NAME: ______________________________

ORGANIZATION: ______________________________

OLD ADDRESS	**CURRENT ADDRESS**
____________	____________
____________	____________
____________	____________

TELEPHONE NUMBER: (   ) ______________________________

DSWA PUBLICATION NUMBER/TITLE	**CHANGES/DELETIONS/ADDITIONS, etc.)** *(Attach Sheet if more Space is Required)*
____________	____________
____________	____________
____________	____________

DSWA OR OTHER GOVERNMENT CONTRACT NUMBER: ______________

CERTIFICATION OF NEED-TO-KNOW BY GOVERNMENT SPONSOR (if other than DSWA):

SPONSORING ORGANIZATION: ______________________________

CONTRACTING OFFICER OR REPRESENTATIVE: ______________________________

SIGNATURE: ______________________________

CUT HERE AND RETURN

DEFENSE SPECIAL WEAPONS AGENCY
ATTN: IMAS
6801 TELEGRAPH ROAD
ALEXANDRIA, VA 22310-3398

DEFENSE SPECIAL WEAPONS AGENCY
ATTN: IMAS
6801 TELEGRAPH ROAD
ALEXANDRIA, VA 22310-3398

ERRATA

for

DSWA-TR-96-46-V1

DAA-Based Computational Boundaries for Ground-Shock Analysis
Volume 1-DAA Formulation and Canonical Comparisons

This document was published with an incorrect report number (DSWA-TR-96-46) on the front cover and block 10 of the SF 298. The number in both places should read DSWA-TR-96-46-V1. Please make pen and ink change in both places to show the correct report number.

REPORT DOCUMENTATION PAGE

Form Approved
OMB No. 0704-0188

1. AGENCY USE ONLY (Leave blank)

2. REPORT DATE
971201

3. REPORT TYPE AND DATES COVERED
Technical 920501 - 950430

4. TITLE AND SUBTITLE
DAA-Based Computational Boundaries for Ground-Shock Analysis, Volume I - DAA Formulation and Canonical Comparisons

5. FUNDING NUMBERS
C - DNA 001-92-C-0038
PE - 62715H
PR - AC
TA - AK
WU - DH00002

6. AUTHOR(S)
Brett A. Lewis and Thomas L. Geers

7. PERFORMING ORGANIZATION NAME(S) AND ADDRESS(ES)
University of Colorado
Mechanical Engineering Department
Campus Box 19
Boulder, CO 80309

8. PERFORMING ORGANIZATION REPORT NUMBER

9. SPONSORING/MONITORING AGENCY NAME(S) AND ADDRESS(ES)
Defense Special Weapons Agency
6801 Telegraph Road
Alexandria, VA 22310-3398
WEL/Giltrud

10. SPONSORING/MONITORING AGENCY REPORT NUMBER
DSWA-TR-96-46

11. SUPPLEMENTARY NOTES
This work was sponsored by the Defense Special Weapons Agency under RDT&E RMC Code B 4662 D AC AK 00002 4300 A AC 25904D.

12a. DISTRIBUTION/AVAILABILITY STATEMENT
Approved for public release; distribution is unlimited.

12b. DISTRIBUTION CODE

13. ABSTRACT (Maximum 200 words)
This document describes the formulation and implementation of a computational boundary for elastic solids based on doubly asymptotic approximations (DAA's). DAA's combine high-frequency (wave propagation) and low-frequency (quasi-static) approximations in a systematic manner to produce a relationship between scattered-wave tractions and displacements on the boundary; this relationship approaches exactness at high and low frequencies and provides a smooth transition between. Second-order DAA's for three-dimensional, linear-elastic infinite and semi-infinite media are developed for implementation into general purpose numerical (finite element or finite difference) programs. In addition, modal DAA's for spherical cavities are developed. Then, DAA results, both general and modal, are compared with analytical and other numerical results for problems involving infinite and semi-infinite media.

14. SUBJECT TERMS
Non Reflecting Boundaries
Doubly Asymptotic Approximations
Elasto Dynamics
Computational Boundary

15. NUMBER OF PAGES
88

16. PRICE CODE

17. SECURITY CLASSIFICATION OF REPORT	18. SECURITY CLASSIFICATION OF THIS PAGE	19. SECURITY CLASSIFICATION OF ABSTRACT	20. LIMITATION OF ABSTRACT
UNCLASSIFIED	UNCLASSIFIED	UNCLASSIFIED	SAR

NSN 7540-01-280-5500

Standard Form 298 (Rev. 2-89)
Prescribed by ANSI Std Z39-18
298-102

CLASSIFIED BY:
N/A Since Unclassified.

DECLASSIFY ON:
N/A Since Unclassified.

SUMMARY

This document describes the formulation and implementation of a computational boundary for elastic solids based on doubly asymptotic approximations (DAA). DAA's combine high-frequency (wave propagation) and low-frequency (quasi-static) approximations in an systematic manner to produce a relationship between scattered-wave tractions and displacements on the boundary; this relationship approaches exactness at high and low frequencies and provides a smooth transition between. Second order DAA's for three-dimensional, linear-elastic infinite and semi-infinite media are developed for implementation into general purpose numerical (finite element or finite difference) programs. In addition, modal DAA's for spherical cavities are developed. Then, DAA results, both general and modal, are compared with analytical and other numerical results for problems involving infinite and semi-infinite media.

TABLE OF CONTENTS

TABLE OF CONTENTS (Continued)

FIGURES

FIGURES (Continued)

SECTION 1

INTRODUCTION

Non-reflecting boundaries for transmitting transient wave energy in an unbounded elastic solid have many applications, including ground shock analysis, earthquake analysis, and quantitative non-destructive evaluation. For example, in a dynamic analysis of a fully or partially buried structure, the structure is of primary concern, but a certain amount of the surrounding soil is typically included in the analysis to treat the soil-structure interaction. Unfortunately, spurious reflections intrude into the calculations when waves scattered from the structure reach a fixed or free soil boundary. This forces the analyst to keep the boundary far from the structure, thereby requiring the inclusion of an large amount of soil. Thus, non-reflecting boundaries, which may be placed relatively close to or directly on the embedded structure, are needed.

Because of the broad spectrum of frequencies that need to be included in many transient dynamics analyses, it is not efficient to employ Fourier transform (time-harmonic) methods. More importantly, when the near-field medium and/or structure respond nonlinearly, time-harmonic methods cannot be used; only transient methods can be used. Doubly Asymptotic Approximations (DAA's) are time-domain non-reflecting boundary relations that match asymptotically the exact elastodynamic integral representation for infinite and semi-infinite domains at both early and late times. For broad-spectrum problems, doubly asymptotic approximations are more robust than singly asymptotic approximations, which only match the exact representations at one limit.

Currently, most non-reflecting boundaries implemented in transient finite-element analysis programs are based on the plane-wave (early-time) approximation(see, e.g., (Whirley, 1991)), which is singly asymptotic. If the problem of interest involves late-time, low-frequency components, the plane-wave boundary will produce incorrect results. However, the second-order DAA derived during this study will reproduce with high fidelity both the early-time and late-time responses, and will reproduce with good accuracy the intermediate-time response.

Underwood and Geers (Underwood and Geers, 1981) heuristically formulated and Mathews and Geers (Mathews and Geers, 1987) developed further the first-order DAA for an infinite domain (DAA_1^W). The goal of the present study has been to formulate and evaluate doubly asymptotic approximations for transient elastodynamic analysis, especially second-order approximations, that have not been previously formulated. The specific objectives under this goal are:

1. Develop the *first-order doubly asymptotic approximation for a homogenous, semi-infinite, elastic domain (a half–space)*: DAA_1^H. To achieve this, a first-order late-time approximation is derived and a systematic operator-matching method is employed to combine the early-time and late-time approximations into DAA_1^H.
2. Develop the *second-order doubly asymptotic approximation for a homogenous, infinite, elastic domain (a whole–space)*: DAA_2^W. To achieve this, second-order approximations for early-time (high frequency) and late-time (low frequency) response in infinite domains are formulated. In addition, a second-order operator matching method is employed to combine the early-time and late-time approximations into DAA_2^W.
3. Develop the *second-order doubly asymptotic approximation for a homogenous, semi-infinite, elastic domain* (a half–space): DAA_2^H. The principal challenge in this effort is determining a second-order late-time (low frequency) approximation for a semi-infinite elastic domain. The same operator-matching method used in the previous component is used to contruct the DAA_2^H.
4. Obtain exact and DAA relations for the dilatational, rotational, and translational motions of a spherical boundary in an infinite elastic medium subjected to transient internal tractions.
5. Compare numerical DAA_1^W, DAA_1^H, DAA_2^W, and DAA_2^H results for selected evaluation problems with those of other investigators. This involves the development of general-purpose computer programs based on the boundary element method. In addition, comparisons are made between the analytical modal results of the previous objective and corresponding results generated with the general-purpose DAA programs.

How these objectives are reached is documented in the following sections. The literature in the field is reviewed in Section 2. In Section 3, the fundamental equations used in this study are presented. Section 4 addresses the first- and second-order early-time (high-frequency) approximations, and Section 5 addresses the first-and second-order late-time (low-frequency) approximations. In Section 6, the first- and the second-order doubly asymptotic approximations are formulated by operator matching.

Section 7 presents exact and DAA relations for breathing and translational motions of a spherical boundary in an infinite elastic medium. In Section 8, various DAA results are compared with results obtained by other means. Finally, Section 9 states the conclusions reached in this study.

SECTION 2

REVIEW OF THE LITERATURE

In this chapter we review previously published work in the field of transient elastodynamics as applied to non-reflecting boundaries. We will concentrate on the theoretical work more than on the numerical work. The numerical aspects, especially for non-reflecting boundaries, may be found in Manolis and Beskos (Manolis and Beskos, 1988).

2.1 ELASTODYNAMIC THEORY.

The foundations of dynamic elasticity were laid by Poisson, Stokes, Kirchhoff, and Love (Poisson, 1820), (Stokes, 1849), (Kirchhoff, 1883), (Love, 1904b), (Love, 1904a), (Love, 1944). Poisson formulated the initial value problem for a dynamic elastic domain in 1819. Poisson's formula results from transforming the wave equation, $\ddot{\phi} = c^2\nabla^2\phi$, into an integral formula that equates the value of ϕ at a point to an integral taken over a sphere surrounding the point. Kirchhoff generalized this formula to equate the value of ϕ at a point to an integral taken over an arbitrary surrounding surface. Stokes established the fundamental singular solution of the equations of elastodynamics in an infinite region due to a time-dependent concentrated body force. Love added to this foundation, proving that certain initial velocity conditions involving continuity had to be met for the integral equations of Poisson and Kirchhoff to be applied properly (Love, 1904b), (Love, 1904a), (Love, 1944).

Doyle (Doyle, 1966), using results from Sternberg and Eubanks (Sternburg and Eubanks, 1957), determined that the fundamental singular integral equations could be simplified by employing the Laplace transform. In addition, Doyle showed that the initial- and boundary-value problems could also be formulated using the Laplace transform. Cruse and Rizzo (Cruse and Rizzo, 1968) extended Doyle's results to the solution of general problems by using boundary element methods in the Laplace transform domain. The drawback of this approach is the difficulty of transform inversion.

If the boundary integral equations are not Laplace transformed, they contain convolutions in time. The solution of geometrically complex problems through the use of time convolution is very computer-resource intensive. Therefore, neither Laplace-transformed nor time-convolved boundary integral equations are suitable for use as non-reflecting boundaries in practical transient elastodynamics analysis (Manolis, 1983).

2.2 NON-REFLECTING BOUNDARIES.

The objective of a non-reflecting boundary in scattering analysis is to completely absorb the scattered waves in order to simulate an infinite domain. Some early work on scattering in an elastic solid was done by Ying and Truell (Ying and Truell, 1956), who formulated a solution for the problem of a plane longitudinal wave scattered by a spherical obstacle in an isotropically elastic solid. This formulation, like so many others (Pow and Mow, 1972), (Uberall and others, 1990), assumes the incident and scattered waves are time harmonic, which, as mentioned above, is not applicable to problems involving non-linear transient response.

A second method used in scattering problems is ray theory (Achenbach and others, 1982). Ray theory has been widely used in electromagnetics, where it is often called geometrical optics. Ray theory employs asymptotic approximations that are accurate for high-frequency response (Achenbach and others, 1982), (Freidlander, 1958). Ray theory was extended by H. B. Keller and by J. B. Keller and his coworkers from electromagnetics and acoustics to elastodynamics (Keller, 1964), (Keller, 1958), (Ahluwalia *et al.*, 1969).

Recently, Givoli and J.B. Keller have developed non-reflecting boundaries for transient elastodynamics (Givoli and Keller, 1990), (Givoli, 1992). These boundaries pertain to a two-dimensional circular geometry, and would be difficult to implement in a general manner. Kallivokas (Kallivokas *et al.*, 1991) have developed a high-frequency (singly asymptotic) non-reflecting boundary for two-dimensional applications that is based on elastodynamic ray theory (Keller, 1958).

Doubly asymptotic approximations were originally developed to treat structures submerged in acoustic media by Geers in the 1970's (Geers, 1971), (Geers, 1978). Since that time, DAA's for acoustic media has been extended and more systematically derived (Felippa, 1980a), (Geers and Felippa, 1983), (Nicholas-Vullierme, 1991), (Geers and Zhang, 1991). A first-order DAA has also been formulated for electromagnetic scattering by Geers and Zhang (Geers and Zhang, 1988). The first-order doubly asymptotic approximation for infinite elastic media was formulated heuristically by Underwood and Geers (Underwood and Geers, 1981), and further developed by Mathews and Geers (Mathews and Geers, 1987). As mentioned previously, doubly asymptotic approximations are much more robust than singly asymptotic approximations.

SECTION 3

FUNDAMENTAL EQUATIONS

In this section we present the fundamental equations that are used to formulate the DAA's. Small characters with arrow accents represent vectors, capital characters represent tensors or matrices, and standard font characters represent scalars.

Let us express the displacement vector $\vec{u}(\vec{x}, t)$ through a Helmholtz decomposition in terms of a scalar potential $\phi(\vec{x}, t)$ and a vector potential $\vec{\psi}$(x,y,z,t) as (see, *e.g.*, (Achenbach, 1973)),

$$\vec{u}(\vec{x}, t) = \nabla\phi(\vec{x}, t) + \nabla \times \vec{\psi}(\vec{x}, t), \qquad \nabla \cdot \vec{\psi}(\vec{x}, t) = 0. \tag{3.1}$$

The wave equation for a uniform elastic medium then separates into the uncoupled wave equations

$$\begin{aligned} c_D^2 \nabla^2 \phi(\vec{x}, t) &= \ddot{\phi}(\vec{x}, t), \\ c_S^2 \nabla^2 \vec{\psi}(\vec{x}, t) &= \ddot{\vec{\psi}}(\vec{x}, t), \end{aligned} \tag{3.2}$$

in which c_D and c_S are the dilatational– and shear–wave speeds, respectively, given by

$$c_D^2 = \frac{\lambda + 2\mu}{\rho}, \qquad c_S^2 = \frac{\mu}{\rho}, \tag{3.3}$$

where λ and μ are the Lame' parameters for the medium. The stress tensor is given by (see, e.g., (Eringen and Suhubi, 1975))

$$\vec{\sigma} = \lambda\nabla^2\phi I + 2\mu\nabla\nabla\phi + \mu(\nabla\nabla \times \vec{\psi} + \nabla \times \vec{\psi}\nabla). \tag{3.4}$$

Where I is the identity tensor.

An exact integral–equation solution to (3.1) and (3.2) on the smooth surface or surfaces of an elastic medium is provided by Love's integral identity, which may be written in Laplace–transform space as (Cruse and Rizzo, 1968)

$$\frac{1}{2}\vec{u}(F,s) + \int_S \vec{u}(P,s)\vec{T}(F,P,s)dS_P = \int_S \vec{t}(P,s)\vec{U}(F,P,s)dS_P. \tag{3.5}$$

In this equation, F is the field point and P is an integration point on the surface S; $\vec{u}(F,s)$ and $\vec{t}(P,s)$ are surface displacement and traction vectors, respectively.

For a whole-space, $\vec{T}(F,P,s)$ and $\vec{U}(F,P,s)$ are second–order tensor operators with components

$$\begin{aligned} U_{ij}(s) &= \frac{1}{4\pi\mu}(\gamma\delta_{ij} - \chi R_{,i}R_{,j}), \\ T_{ij}(s) &= \frac{1}{4\pi}[(\frac{d\gamma}{dR} - \frac{1}{R}\chi)(\delta_{ij}\frac{\partial R}{\partial n} + R_{,j}n_i) \\ &\quad -\frac{2}{R}\chi(n_jR_{,i} - 2R_{,i}R_{,j}\frac{\partial R}{\partial n}) - 2\frac{d\chi}{dR}R_{,i}R_{,j}\frac{\partial R}{\partial n} \\ &\quad +(\frac{c_D^2}{c_T^2} - 2)(\frac{d\gamma}{dR} - \frac{d\chi}{dR} - \frac{2}{R}\chi)R_{,i}n_j], \end{aligned} \tag{3.6}$$

where the usual Cartesian tensor notation applies, R is defined as $\mid \vec{r}_P - \vec{r}_F \mid$, and where $\psi(R,s)$ and $\chi(R,s)$ are given for three dimensions as:

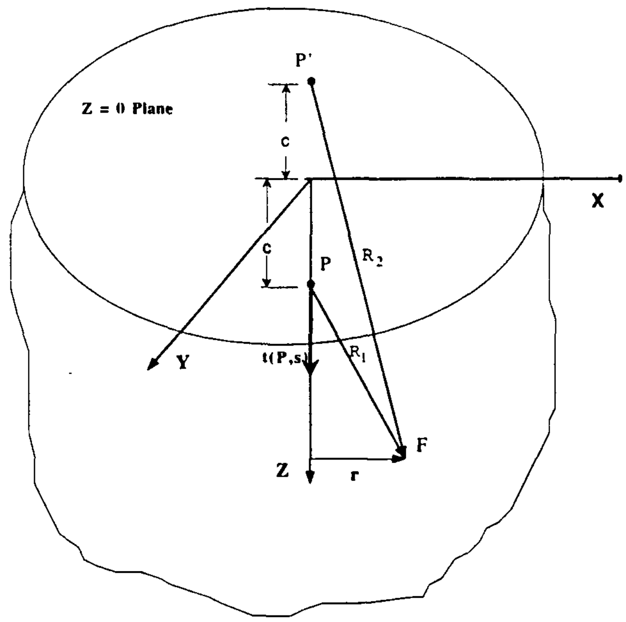

Figure 3-1. Description of semi-infinite domain for force normal to surface.

$$\gamma(R,s) = (1+\frac{c_S}{sR}+\frac{c_S^2}{s^2R^2})\frac{e^{-sR/c_S}}{R} - \frac{c_S^2}{c_D^2}(\frac{c_D}{sR}+\frac{c_D^2}{s^2R^2})\frac{e^{-sR/c_D}}{R}$$

$$\chi(R,s) = (1+\frac{3c_S}{sR}+\frac{3c_S^2}{s^2R^2})\frac{e^{-sR/c_S}}{R} - \frac{c_S^2}{c_D^2}(1+\frac{3c_D}{sR}+\frac{3c_D^2}{s^2R^2})\frac{e^{-sR/c_D}}{R}. \tag{3.7}$$

The second-order tensor operators used in equation (3.5) for a half–space have been derived previously by Banerjee and Mamoon (Banerjee and Mamoon, 1990). The first group of operators is based on a force vector normal to the half-space boundary, and the second group is based on a force vector parallel to the boundary. Figure 3-1 shows the coordinate system and the other geometric quantities used for the first group of operators , which obviously pertain to an axisymtric problem. The notation used is that of Banerjee and Mamoon.

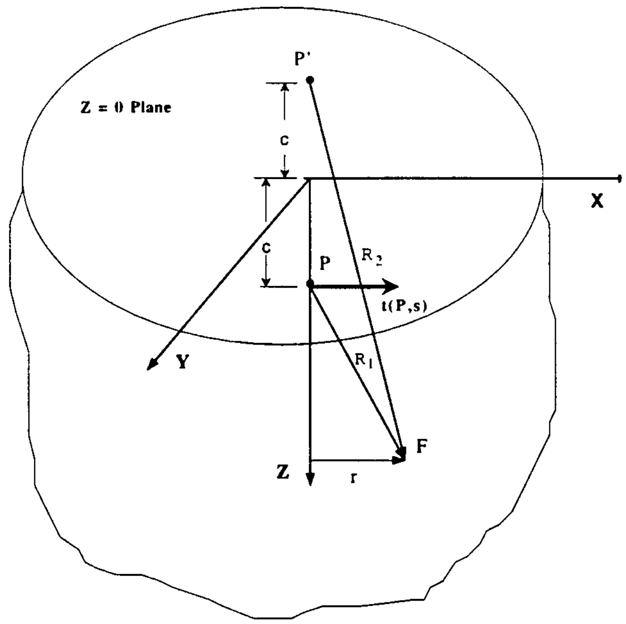

Figure 3-2. Description of semi-infinite domain for force parallel to surface.

The operator components pertain to the following point forces:

1. Single dynamic force at (0,0,+c)
2. Single dynamic force at (0,0,-c)
3. Dynamic double forces at (0,0,-c)
4. Dynamic centre of compression at (0,0,-c)
5. Line of dynamic centers of compression extending from $z = -c$ to $z = -\infty$
6. Dynamic doublet at (0,0,-c)

The resulting operator components are given the appendix.

Figure 3-2 shows the coordinate system for the second group of operators. The point forces consist of

1. Single dynamic force at (0,0,+c)
2. Single dynamic force at (0,0,-c)

3. Dynamic double force with moment at (0,0,-c)
4. Line of dynamic double forces with moment extending from $z = -c$ to $z = -\infty$
5. Dynamic doublets at (0,0,-c)
6. Line of dynamic doublets extending from $z = -c$ to $z = -\infty$ with strength proportional to the distance from $z = -c$

The resulting operator components are given in the appendix.

The U^1 components in (A.1) and (A.2) are identical to those of the first of (3.6), which is the standard Kelvin solution for a point force in an infinite elastic space. The other terms are additional terms to be added to the basic Kelvin solution to form the half–space solution (Brebbia and others, 1984). The $\vec{T}$ operators for the half-space are found from (A.1) and (A.2) by differentiating the $\vec{U}$ components with respect to spatial coordinates (Brebbia and others, 1984). The operators (A.1), based on the cylindrical coordinate system, are transformed to the Cartesian coordinate system using standard tensor techniques for coordinate transformations.

SECTION 4

EARLY–TIME APPROXIMATIONS

Early-time approximations are non-reflecting boundary relations valid for $ct \ll a$, where a is a characteristic dimension of the boundary S and c is a wave speed (Felippa, 1980b). *The approximations are local*; they depend only on geometrical information in the neighborhood of the field point F. Thus, early-time approximations for an infinite domain (whole–space) are identical to those for a semi-infinite domain (half–space).

We present herein two derivations of early-time approximations. The first derivation is based on ray elastodynamics (Keller (Keller, 1958)). The second is based on work by Felippa (Felippa, 1980b) for an acoustic medium, which is in turn based on Kirchhoff's retarded potential formula (Kirchhoff, 1883). The two derivations produce the same relationships involving the displacement potentials. Those relationships are then used to formulate two early-time approximations (ETA's) involving tractions and displacements.

4.1 RAY ELASTODYNAMICS DERIVATION.

In this section we present the first method for deriving the early-time approximations. This derivation is accomplished using ray elastodynamic theory developed by J.B Keller and H.B. Keller (Keller, 1964), (Ahluwalia *et al.*, 1969), (Achenbach and others, 1982). The basic assumption of ray elastodynamics is that disturbances are propagated along rays to which the disturbance surface, *i.e.* the wavefront, is always normal. Figure 4-1 shows the basic geometry.

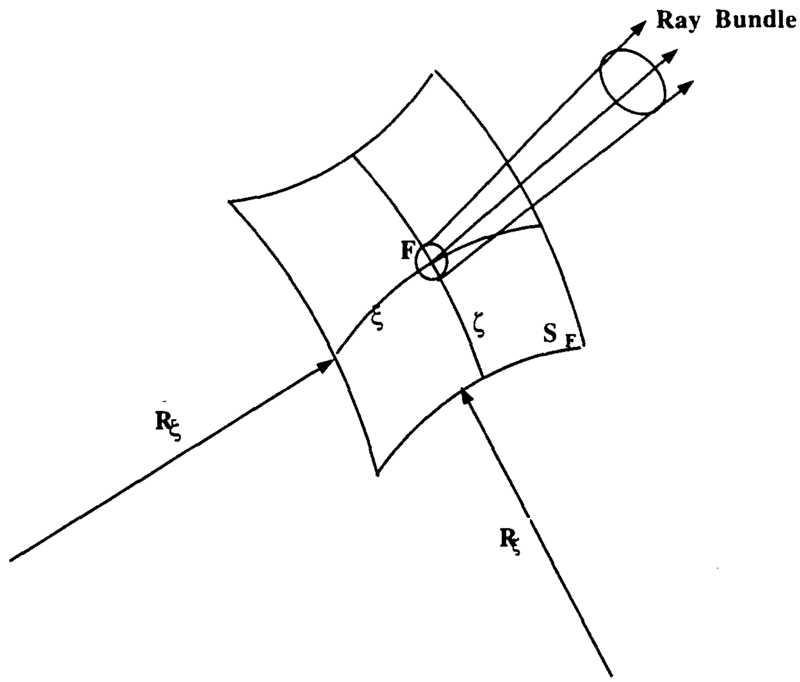

Figure 4-1. Definition of ray bundle for elastodynamics.

The potentials in (3.1) may be represented by a ray series (Ahluwalia *et al.*, 1969)

$$\phi(\vec{x}, s) \;=\; \exp[-s\varphi(\vec{x})/c_D] 0_{m=0}^{\infty} (\frac{-s}{c_D})^{-(m+1)} \Phi^m(\vec{x})$$

$$\vec{\psi}(\vec{x}, s) \;=\; \exp[-s\varphi(\vec{x})c_S] 0_{m=0}^{\infty} (\frac{-s}{c_S})^{-(m+1)} \Psi^m(\vec{x}), \tag{4.1}$$

where the phase function $\varphi(\vec{x})$ and the amplitude functions $\Phi^m(\vec{x})$ and $\Psi^m(\vec{x})$ depend on the spatial variables, but are independent of s, the Laplace transform parameter. Keller (Keller, 1964) has shown that, at *high frequencies*, the displacement potentials can be adequately described with only the first term in each expansion (4.1) as

$$\begin{aligned} \phi(F,\eta,s) &\approx \exp[-s\eta/c_D]\left[\frac{R_\xi R_\zeta}{(\eta+R_\xi)(\eta+R_\zeta)}\right]^{\frac{1}{2}}\phi(F,0,s) \\ \vec{\psi}(F,\eta,s) &\approx \exp[-s\eta/c_S]\left[\frac{R_\xi R_\zeta}{(\eta+R_\xi)(\eta+R_\zeta)}\right]^{\frac{1}{2}}\vec{\psi}(F,0,s), \end{aligned} \tag{4.2}$$

where the argument 0 denotes the initial wavefront on the surface, R_ξ and R_ζ are the principal radii of curvature of the initial surface, and η is the coordinate along the ray, which is orthogonal to each wavefront and straight for homogenous media. Equation 4.2 relates the displacement potentials at some point η along the ray to the initial disturbance surface, and to the initial amplitude functions $\phi(F,0,s)$ and $\vec{\psi}(F,0,s)$.

At a field point F on the surface, the ray is directed along the normal to the surface. Therefore, taking derivatives of ϕ with respect to the local coordinates at F, we obtain

$$\begin{aligned} \frac{\partial\phi}{\partial n}(F,\eta,s) &\approx -\frac{s}{c_D}\exp[-s\eta/c_D]\left[\frac{R_\xi R_\zeta}{(\eta+R_\xi)(\eta+R_\zeta)}\right]^{\frac{1}{2}}\phi(F,0,s) \\ &- \frac{1}{2}exp[-s\eta/c_D]\frac{R_\xi R_\zeta(2\eta+R_\xi+R_\zeta)}{(\eta+R_\xi)^2(\eta+R_\zeta)^2}\left[\frac{(\eta+R_\xi)(\eta+R_\zeta)}{R_\xi R_\zeta}\right]^{\frac{1}{2}}\phi(F,0,s), \\ \frac{\partial\phi}{\partial\zeta} &\approx 0, \\ \frac{\partial\phi}{\partial\xi} &\approx 0. \end{aligned} \tag{4.3}$$

From the first of these, the partial derivative of ϕ with respect to the local normal at the point F on the surface is just

$$\frac{\partial \phi}{\partial n}(F,0,s) = \lim_{\eta \to 0} \frac{\partial \phi}{\partial n}(F,\eta,s) \approx \left(\frac{-s}{c_D} - \frac{R_\xi + R_\zeta}{2R_\xi R_\zeta}\right)\phi(F,0,s)$$

$$= -\left(\frac{s}{c_D} + \kappa\right)\phi(F,0,s), \tag{4.4}$$

where κ is the mean curvature (positive when the surface is convex). In (4.4), the derivative of the scalar potential at point F is related to the scalar potential itself at the same point F. We can readily obtain a similar result for the vector potential $\vec{\psi}$. Thus we have the following results for the partial derivatives of the displacement potentials with respect to the local coordinates at point F:

$$\begin{aligned}
\frac{\partial \phi}{\partial n}(F,s) &\approx -\left(\frac{s}{c_D} + \kappa\right)\phi(F,s) \\
\frac{\partial \vec{\psi}}{\partial n}(F,s) &= -\left(\frac{s}{c_S} + \kappa\right)\vec{\psi}(F,s) \\
\frac{\partial \phi}{\partial \xi}(F,s) &\approx 0 \\
\frac{\partial \vec{\psi}}{\partial \xi}(F,s) &\approx 0 \\
\frac{\partial \phi}{\partial \zeta}(F,s) &\approx 0 \\
\frac{\partial \vec{\psi}}{\partial \zeta}(F,s) &\approx 0.
\end{aligned} \tag{4.5}$$

These results are used below to form early-time approximations.

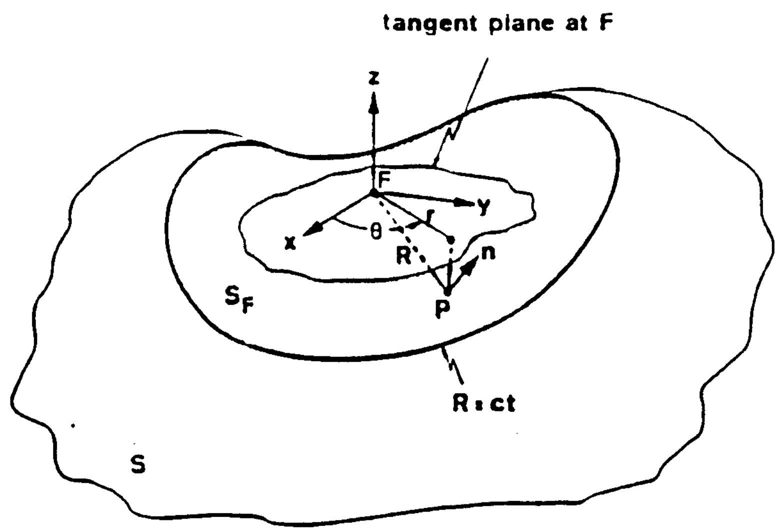

Figure 4-2. Coordinate systems on surface for early-time approximations.

4.2 RETARDED POTENTIAL DERIVATION.

In this section we develop the elastodynamic equivalents to Felippa's first two early-time approximations for acoustic media (Felippa, 1980b). We use two local coordinate systems, as seen in Figure 4-2. The first is a Cartesian system centered at point F, where x and y define the plane tangent to the surface at F. At point F, x and y coincide with the orthogonal surface coordinates ξ and ζ. The second coordinate system is a cylindrical system (r, θ, z) with $r^2 = x^2 + y^2$.

The distance between the field point F and the integration point P is given by R, which is $R = \sqrt{r^2 + z^2}$. Felippa expanded the z coordinate of the surface in a Taylor series about the point F to get

$$z = AR^2 + BR^3 + (C - A^3)R^4 + (D - \frac{7}{2}A^2B)R^5 + \cdots . \tag{4.6}$$

where

$$
\begin{aligned}
A &= \frac{\partial^2 z}{\partial x^2}\cos^2\theta + \frac{\partial^2 z}{\partial x \partial y}\sin\theta\cos\theta + \frac{\partial^2 z}{\partial y^2}\sin^2\theta \\
B &= \frac{\partial^3 z}{\partial x^3}\cos^3\theta + 3\frac{\partial^3 z}{\partial x \partial x \partial y}\sin\theta\cos^2\theta + \cdots \frac{\partial^3 z}{\partial y^3}\sin^3\theta \qquad (4.7) \\
& \cdots,
\end{aligned}
$$

The derivatives $\frac{\partial z}{\partial x}, \ldots$ are assumed to exist at F, i.e., the surface is smooth.

First, we discuss irrotational motion. The integral solution to the wave equation for the scalar displacement potential ϕ is

$$
2\pi\phi(F,t) = \int_S \left\{ R^{-1}\frac{\partial\phi(P,t_R)}{\partial n} + R^{-2}\frac{\partial R}{\partial n}\left(\phi(P,t_R) + \frac{R}{c_D}\dot{\phi}(P,t_R)\right)\right\} dS_P, \qquad (4.8)
$$

which is Kirchhoff's retarded potential formula (Love, 1904a), (Eringen and Suhubi, 1975), where $t_R = t - R/c_D$ represents the retarded time.

We expand ϕ about the field point F in a Taylor series to get

$$
\begin{aligned}
\phi(P,t) &= \phi(F,t) + \frac{\partial\phi}{\partial\xi}(F,t)\,\xi + \frac{\partial\phi}{\partial\zeta}(F,t)\,\zeta + \frac{1}{2}\frac{\partial^2\phi}{\partial\xi^2}(F,t)\,\xi^2 \\
& \qquad\qquad (4.9) \\
&+ \frac{\partial^2\phi}{\partial\xi\partial\zeta}(F,t)\,\xi\zeta + \frac{1}{2}\frac{\partial^2\phi}{\partial\zeta^2}(F,t)\,\zeta^2 + \cdots.
\end{aligned}
$$

At F, the coordinates ξ and ζ coincide with the x and y coordinates, and can be approximated as

$$
\xi = R\cos\theta[1 + O(R^2)], \;\; \zeta = R\sin\theta[1 + O(R^2)] \qquad (4.10)
$$

Therefore,

$$\begin{aligned}
\phi(P,t) &= \phi(F,t) + \frac{\partial \phi}{\partial x}(F,t)\, R\cos\theta[1+O(R^2)] + \frac{\partial \phi}{\partial y}(F,t)\, R\sin\theta[1+O(R^2)] \\
&\quad + \left\{ \frac{1}{2}\frac{\partial^2 \phi}{\partial x^2}(F,t)\, \cos^2\theta + \frac{\partial^2 \phi}{\partial x \partial y}(F,t)\, \cos\theta\sin\theta \right. \\
&\qquad \left. + \frac{1}{2}\frac{\partial^2 \phi}{\partial y^2}(F,t)\, \sin^2\theta \right\} R^2[1+O(R^2)] + \cdots .
\end{aligned} \tag{4.11}$$

The normal derivative of ϕ may be similarly expanded to obtain

$$\begin{aligned}
\frac{\partial \phi}{\partial n}(P,t) &= \frac{\partial \phi}{\partial n}(F,t) + \frac{\partial^2 \phi}{\partial n \partial x}(F,t)\, R\cos\theta[1+O(R^2)] \\
&\quad + \frac{\partial^2 \phi}{\partial n \partial y}(F,t)\, R\sin\theta[1+O(R^2)] \\
&\quad + \left\{ \frac{1}{2}\frac{\partial^3 \phi}{\partial n \partial x^2}(F,t)\, \cos^2\theta + \frac{\partial^3 \phi}{\partial n \partial x \partial y}(F,t)\, \cos\theta\sin\theta \right. \\
&\qquad \left. + \frac{1}{2}\frac{\partial^3 \phi}{\partial n \partial y^2}(F,t)\, \sin^2\theta \right\} R^2[1+O(R^2)] + \cdots .
\end{aligned} \tag{4.12}$$

We now introduce (4.11) and (4.12) into (4.8) and utilize Felippa's expansions for $R^{-1}dS$ and $R^{-2}\frac{\partial R}{\partial n}dS$, viz,

$$\begin{aligned}
R^{-1}dS &= (1 + \frac{1}{2}A_\theta^2 R^2 + \cdots)dR d\theta \\
R^{-2}\frac{\partial R}{\partial n}dS &= -(A + 2BR + 3(C - A^3)R^2 + \cdots)dR d\theta
\end{aligned} \tag{4.13}$$

to obtain

$$2\pi\phi(F,t) \approx \int_0^{c_D t}\int_0^{2\pi} \frac{\partial\phi}{\partial n}(F,t_R)d\theta dR$$

$$+\int_0^{c_D t}\int_0^{2\pi}\left\{\phi(F,t_R)+\frac{R}{c_D}\dot{\phi}(F,t_R)\right\}(-A)d\theta dR. \tag{4.14}$$

Note that $\phi(F,t_R)$ and its normal derivative are functions only of the retarded time t_R and not the coordinates R and θ.

Next, we integrate over θ and divide through by 2π to get

$$\phi(F,t) \approx \int_0^{c_D t}\frac{\partial\phi}{\partial n}(F,t_R)dR - \kappa\int_0^{c_D t}\left\{\phi(F,t_R)+\frac{R}{c_D}\dot{\phi}(F,t_R)\right\}dR \tag{4.15}$$

where κ is again the mean curvature of the surface at F. Then, making the variable change, $R = c_D(t - t_R)$, we get

$$\phi(F,t) \approx c_D\int_0^t \frac{\partial\phi}{\partial n}(F,t_R)dt_R - c_D\kappa\int_0^t\left\{\phi(F,t_R)+(t-t_R)\frac{\partial\phi(F,t_R)}{\partial t_R}\right\}dt_R. \tag{4.16}$$

Finally, integrating by parts and noting that $\phi(F,0) = 0$ for quiescent initial conditions, we obtain

$$\dot{\phi}(F,t) + \kappa c_D\phi(F,t) \approx -c_D\frac{\partial\phi}{\partial n}(F,t). \tag{4.17}$$

which, when transformed to the Laplace transform domain, gives

$$(s+\kappa c_D)\phi(F,s) \approx -c_D\frac{\partial\phi}{\partial n}(F,s). \tag{4.18}$$

We observe that this is identical to the first of (4.5)

Now we consider solenoidal (rotational) motion. The integral solution to the wave equation for the vector potential $\vec{\psi}$ is

$$
\begin{aligned}
2\pi\vec{\psi}(F,t) &= \int_S \left\{ R^{-1}\frac{\partial\vec{\psi}}{\partial n}(P,t_R) \right. \\
&\left. +R^{-2}\frac{\partial R}{\partial n}\left(\vec{\psi}(P,t_R)+\frac{R}{c_S}\dot{\vec{\psi}}(P,t_R)\right)\right\} dS.
\end{aligned}
\tag{4.19}
$$

This is again Kirchhoff's retarded potential formula (Eringen and Suhubi, 1975). Thus, application to $\vec{\psi}$ of the procedure described between (4.8) and (4.18) yields

$$
(s+\kappa c_S)\vec{\psi}(F,s) = -c_S\frac{\partial\vec{\psi}}{\partial n}(F,s). \tag{4.20}
$$

We observe that this is identical to the second of (4.5).

4.3 FORMULATION OF ETA$_2$.

In this section we employ (4.5) to obtain early-time relations between surface tractions and displacements that do not involve spatial derivatives. For (4.5) we used a local curvilinear coordinate system ξ, ζ, n with the origin at point F, characterized by two principal curvatures, R_ξ and R_ζ (Figure 4-1). Thus we can write $\xi = R_\xi\theta_1$ and $\zeta = R_\zeta\theta_2$, so that our metric coefficients are $h_1 = R_\xi$, $h_2 = R_\zeta$, and $h_3 = 1$. We also note that, because the spatial derivatives of the scalar and vector potentials are non-negligible only for the normal direction, we have the early-time surface formulas (Moon and Spencer, 1961)

$$
\begin{aligned}
\nabla\phi &\approx \frac{\partial\phi}{\partial n}\mathbf{k} \\
\nabla\times\vec{\psi} &\approx -\left(\frac{\partial\psi_\zeta}{\partial n}+R_\zeta^{-1}\psi_\zeta\right)\mathbf{i}+\left(\frac{\partial\psi_\xi}{\partial n}+R_\xi^{-1}\psi_\xi\right)\mathbf{j} \\
\nabla^2\vec{\psi} &= \nabla(\nabla\cdot\vec{\psi})-\nabla\times\nabla\times\vec{\psi} \\
&\approx \left[\frac{\partial^2\psi_\xi}{\partial n^2}+2\kappa\frac{\partial\psi_\xi}{\partial n}+(R_\xi-R_\zeta)R_\zeta^{-1}R_\xi^{-2}\psi_\xi\right]\mathbf{i} \\
&\quad +\left[\frac{\partial^2\psi_\zeta}{\partial n^2}+2\kappa\frac{\partial\psi_\zeta}{\partial n}+(R_\zeta-R_\xi)R_\zeta^{-2}R_\xi^{-1}\psi_\zeta\right]\mathbf{j} \\
\nabla^2\phi &\approx \frac{\partial^2\phi}{\partial n^2}+2\kappa\frac{\partial\phi}{\partial n} \qquad (4.21)
\end{aligned}
$$

$$
\nabla\nabla\phi \approx \begin{pmatrix} 0 & 0 & 0 \\ 0 & 0 & 0 \\ 0 & 0 & \frac{\partial^2\phi}{\partial n^2} \end{pmatrix}
$$

$$
\nabla(\nabla\times\vec{\psi})+(\nabla\times\vec{\psi})\nabla\approx
$$

$$
\begin{pmatrix}
0 & 0 & -\frac{\partial^2\psi_\zeta}{\partial n^2}-R_\zeta^{-1}\frac{\partial\psi_\zeta}{\partial n}+R_\zeta^{-2}\psi_\zeta \\
0 & 0 & \frac{\partial^2\psi_\xi}{\partial n^2}+R_\xi^{-1}\frac{\partial\psi_\xi}{\partial n}-R_\xi^{-2}\psi_\xi \\
-\frac{\partial^2\psi_\zeta}{\partial n^2}-R_\zeta^{-1}\frac{\partial\psi_\zeta}{\partial n}+R_\zeta^{-2}\psi_\zeta & \frac{\partial^2\psi_\xi}{\partial n^2}+R_\xi^{-1}\frac{\partial\psi_\xi}{\partial n}-R_\xi^{-2}\psi_\xi & 0
\end{pmatrix}
$$

We obtain the early-time displacement-potential surface relations by introducing the first two of (4.21) into (3.1), which yields

$$
\begin{aligned}
u_n &\approx \frac{\partial \phi}{\partial n}, \\
u_\xi &\approx -\frac{\partial \psi_\zeta}{\partial n} - R_\zeta^{-1}\psi_\zeta \\
u_\zeta &\approx \frac{\partial \psi_\xi}{\partial n} + R_\xi^{-1}\psi_\xi .
\end{aligned}
\tag{4.22}
$$

We obtain the early-time traction-potential surface relations by introducing the last three of (4.21) into (3.4) and defining surface tractions t_n, t_ξ, and t_ζ as the negatives of σ_{nn}, $\sigma_{n\xi}$, and $\sigma_{n\zeta}$ on the surface; this yields

$$
\begin{aligned}
t_n &\approx -(\rho c_D^2 \frac{\partial^2 \phi}{\partial n^2} + 2\kappa\lambda \frac{\partial \phi}{\partial n}) \\
t_\xi &\approx \rho c_S^2 (\frac{\partial^2 \psi_\zeta}{\partial n^2} + R_\zeta^{-1}\frac{\partial \psi_\zeta}{\partial n} - R_\zeta^{-2}\psi_\zeta) \\
t_\zeta &\approx -\rho c_S^2 (\frac{\partial^2 \psi_\xi}{\partial n^2} + R_\xi^{-1}\frac{\partial \psi_\xi}{\partial n} - R_\xi^{-2}\psi_\xi).
\end{aligned}
\tag{4.23}
$$

Also, we obtain early-time surface relations between the potentials and their normal derivatives by introducing the third and fourth of (4.21) into (3.2) and applying the Laplace transform for quiescent initial conditions to get

$$
\begin{aligned}
\frac{s^2}{c_D^2}\phi &\approx \frac{\partial^2 \phi}{\partial n^2} + 2\kappa \frac{\partial \phi}{\partial n} \\
\frac{s^2}{c_S^2}\psi_\xi &\approx \frac{\partial^2 \psi_\xi}{\partial n^2} + 2\kappa \frac{\partial \psi_\xi}{\partial n} + (R_\xi - R_\zeta) R_\zeta^{-1} R_\xi^{-2} \psi_\xi \\
\frac{s^2}{c_S^2}\psi_\zeta &\approx [\frac{\partial^2 \psi_\zeta}{\partial n^2} + 2\kappa \frac{\partial \psi_\zeta}{\partial n} + (R_\zeta - R_\xi) R_\zeta^{-2} R_\xi^{-1} \psi_\zeta].
\end{aligned}
\tag{4.24}
$$

With (4.5) and (4.22) - (4.24) in place, we may now proceed to derive the desired early-time relations.

First, we eliminate ϕ in the first (4.5) by introducing the first of (4.24), eliminate $\frac{\partial^2 \phi}{\partial n^2}$ in the resulting equation by introducing the first of (4.23), eliminate $\frac{\partial \phi}{\partial n}$ in the resulting equation by introducing the first of (4.22), and make use of the first of (3.3); this yields

$$(s + \kappa c_D) t_n = (\rho c_D s + 4\mu\kappa) s u_n, \tag{4.25}$$

where terms of $O(s^0)$ on the right side have been dropped.

We find the early-time stress-displacement relations involving the shear stresses by first using the second of (4.5) to eliminate $\frac{\partial \psi_\xi}{\partial n}$ and $\frac{\partial \psi_\zeta}{\partial n}$ in the last two of (4.24), which yields

$$\begin{aligned}
\frac{\partial^2 \psi_\xi}{\partial n^2} &\approx [s^2 c_S^{-2} + 2\kappa(s c_S^{-1} + \kappa) - R_\xi^{-1}(R_\zeta^{-1} - R_\xi^1)]\psi_\xi \\
\frac{\partial^2 \psi_\zeta}{\partial n^2} &\approx [s^2 c_S^{-2} + 2\kappa(s c_S^{-1} + \kappa) - R_\zeta^{-1}(R_\xi^{-1} - R_\zeta^1)]\psi_\xi.
\end{aligned} \tag{4.26}$$

Second, we use the second of (4.5) again to eliminate $\frac{\partial \psi_\xi}{\partial n}$ and $\frac{\partial \psi_\zeta}{\partial n}$ in the last two of (4.23), which yields

$$\begin{aligned}
t_\xi &\approx \rho c_S^2 [\frac{\partial^2 \psi_\zeta}{\partial n^2} - R_\zeta^{-1}(s c_S^{-1} + \kappa + R_\zeta^{-1})\psi_\zeta] \\
t_\zeta &\approx -\rho c_S^2 [\frac{\partial^2 \psi_\xi}{\partial n^2} - R_\xi^{-1}(s c_S^{-1} + \kappa + R_\xi^{-1})\psi_\xi].
\end{aligned} \tag{4.27}$$

Third, we eliminate $\frac{\partial^2 \psi_\xi}{\partial n^2}$ and $\frac{\partial^2 \psi_\zeta}{\partial n^2}$ in (4.27) by introducing (4.26) to get

$$t_\xi \approx \rho c_S^2[s^2 c_S^{-2} + (2\kappa - R_\zeta^{-1}) s c_S^{-1} + 2\{\kappa^2 - R_\xi^{-1}(R_\zeta^{-1} - R_\xi^{-1})\}$$
$$-R_\zeta^{-1}(\kappa + R_\zeta^{-1})]\psi_\zeta$$
(4.28)
$$t_\zeta \approx -\rho c_S^2[s^2 c_S^{-2} + (2\kappa - R_\xi^{-1}) s c_S^{-1} + 2\{\kappa^2 - R_\zeta^{-1}(R_\xi^{-1} - R_\zeta^{-1})\}$$
$$-R_\xi^{-1}(\kappa + R_\xi^{-1})]\psi_\xi.$$

Fourth, we use the second of (4.5) a third time to eliminate $\frac{\partial \psi_\xi}{\partial n}$ and $\frac{\partial \psi_\zeta}{\partial n}$ in the last two of (4.22), which yields

$$u_\xi \approx (s c_S^{-1} + \kappa - R_\zeta^{-1})\psi_\zeta$$
(4.29)
$$u_\zeta \approx -(s c_S^{-1} + \kappa - R_\xi^{-1})\psi_\xi.$$

Fifth, we eliminate ψ_ξ and ψ_ζ in (4.28) by introducing (4.29) to obtain

$$(s + \beta c_S) t_\xi \approx \rho c_S (s^2 + R_\xi^{-1} c_S s + \beta R_\xi^{-1}) u_\xi$$
(4.30)
$$(s - \beta c_S) t_\zeta \approx \rho c_S (s^2 + R_\zeta^{-1} c_S s - \beta R_\zeta^{-1}) u_\xi,$$

where $\beta = \kappa - R_\zeta^{-1} = -(\kappa - R_\xi^{-1})$.

The traction-displacement relations (4.30) are not quite in proper form. Thus, we multiply the first of (4.30) by ${(s+\kappa c_S)}/{(s+\beta c_S)}$ and the second by ${(s+\kappa c_S)}/{(s-\beta c_S)}$ to get

$$
\begin{aligned}
(s+\kappa c_S)t_\xi &\approx \rho c_S \frac{s+\kappa c_S}{s+\beta c_S}(s^2 + R_\xi^{-1} c_S s)u_\xi \\
(s+\kappa c_S)t_\zeta &\approx \rho c_S \frac{s+\kappa c_S}{s-\beta c_S}(s^2 + R_\zeta^{-1} c_S s)u_\zeta,
\end{aligned}
\tag{4.31}
$$

where terms of $O(s^0)$ on the right side have been dropped. Finally, we employ long division and retain terms only in s^2 and s to obtain

$$
\begin{aligned}
(s+\kappa c_S)t_\xi &\approx [\rho c_S s + 2\kappa\mu] s u_\xi \\
(s+\kappa c_S)t_\zeta &\approx [\rho c_S s + 2\kappa\mu] s u_\zeta
\end{aligned}
\tag{4.32}
$$

The desired relations (4.25) and (4.32) may be assembled to produce the second-order early-time approximation ETA_2 for an elastic medium:

$$
\begin{aligned}
(s+\kappa c_D)t_n &= (\rho c_D s + 4\mu\kappa) s u_n \\
(s+\kappa c_S)t_\xi &= (\rho c_S s + 2\mu\kappa) s u_\xi \\
(s+\kappa c_S)t_\zeta &= (\rho c_S s + 2\mu\kappa) s u_\zeta
\end{aligned}
\tag{4.33}
$$

These are immediately inverse-transformed to obtain the ETA_2 in the time domain:

$$
\begin{aligned}
\dot{t}_n + \kappa c_D t_n &= \rho c_D \ddot{u}_n + 4\mu\kappa \dot{u}_n \\
\dot{t}_\xi + \kappa c_S t_\xi &= \rho c_S \ddot{u}_\xi + 2\mu\kappa \dot{u}_\xi \\
\dot{t}_\zeta + \kappa c_S t_\zeta &= \rho c_S \ddot{u}_\zeta + 2\mu\kappa \dot{u}_\zeta
\end{aligned}
\tag{4.34}
$$

which may be written

$$\dot{\vec{t}}(F,t) + \kappa\vec{C}\vec{t}(F,t) \;=\; \rho\vec{C}\ddot{\vec{u}}(F,t) + \kappa\vec{\Lambda}\dot{\vec{u}}(F,t) \tag{4.35}$$

where

$$\vec{C} = \begin{bmatrix} c_D & & \\ & c_S & \\ & & c_S \end{bmatrix}, \quad \vec{\Lambda} = \begin{bmatrix} 4\mu & & \\ & 2\mu & \\ & & 2\mu \end{bmatrix} \tag{4.36}$$

For very early times ($s \to \infty$) the second order ETA obviously reduces to the first-order ETA

$$\vec{t}(F,t) \;=\; \rho\vec{C}\dot{\vec{u}}(F,t) \tag{4.37}$$

We have completed the formulation of the early–time (high–frequency) approximations ETA_1 and ETA_2. These approximations are commonly called the plane wave and curved wave approximations, respectively. A key property of these approximations is that the coefficient matrices are diagonal; therefore, the approximations are spatially local with uncoupled local components.

We now rotate the early-time approximations from local coordinates to global coordinates. Displacements and tractions in local coordinates can be rotated into global coordinates as

$$\begin{aligned} \vec{u}(F,t) &= \vec{Q}(F)\underline{\vec{u}}(F,t) \\ \vec{t}(F,t) &= \vec{Q}(F)\underline{\vec{t}}(F,t), \end{aligned} \tag{4.38}$$

where $\vec{Q}$ is the rotation tensor. Then (4.37) becomes

$$\vec{Q}\underline{\vec{t}}(F,t) = \rho\vec{C}\vec{Q}\dot{\underline{\vec{u}}}(F,t), \tag{4.39}$$

which yields ETA$_1$ in global coordinates:

$$\vec{\underline{t}}(F,t) = \rho\vec{\underline{C}}\;\dot{\vec{\underline{u}}}(F,t), \tag{4.40}$$

where, because $\vec{Q}^{-1} = \vec{Q}^T$, $\vec{\underline{C}} = \vec{Q}^T\vec{C}\vec{Q}$. The corresponding first-order high-frequency approximation is therefore

$$\vec{\underline{t}}(F,s) = \rho\vec{\underline{C}}s\;\vec{\underline{u}}(F,s), \tag{4.41}$$

The second-order early-time approximation can be similarly rotated to get ETA$_2$ in global coordinates:

$$\dot{\vec{\underline{t}}}(F,t) + \kappa\vec{\underline{C}}\;\vec{\underline{t}}(F,t) \quad = \quad \rho\vec{\underline{C}}\;\ddot{\vec{\underline{u}}}(F,t) + \kappa\vec{\underline{\Lambda}}\;\dot{\vec{\underline{u}}}(F,t), \tag{4.42}$$

where $\vec{\underline{\Lambda}} = \vec{Q}^T\vec{\Lambda}\vec{Q}$. Hence the second-order high-frequency approximation is

$$(s + \kappa\vec{\underline{C}})\vec{\underline{t}}(F,s) = (\rho\vec{\underline{C}}s + \kappa\vec{\underline{\Lambda}})s\vec{\underline{u}}(F,s) \tag{4.43}$$

From this point we will work in global coordinates only; the underlines will be dropped with the understanding that all quantities are global.

SECTION 5

LATE–TIME APPROXIMATIONS FOR ELASTIC DOMAINS

Late-time approximations pertain to low-frequency response, for which the chacteristic elastodynamic wavelengths c_D/f and c_S/f are much larger than the characteristic dimension of the boundary. We will derive first the late time approximations (LTA's) for the infinite domain (whole–space) and then derive the LTA's for the semi-infinite domain (half–space).

5.1 LATE-TIME APPROXIMATIONS FOR A WHOLE–SPACE.

We use (3.5) - (3.7) to construct an approximation that approaches the exact solution as $s \longrightarrow 0$. First, we expand (3.7) in Taylor series as

$$\begin{aligned}\gamma(R,s) &= \frac{1}{2R}(\frac{c_S^2}{c_D^2}+1)-\frac{1}{3}(\frac{c_S^2}{c_D^3}+\frac{2}{c_S})s+\frac{R}{8}(\frac{c_S^2}{c_D^4}+\frac{3}{c_S^2})s^2+O(s^3),\\ \chi(R,s) &= \frac{1}{2R}(\frac{c_S^2}{c_D^2}-1)+\frac{R}{8}(-\frac{c_S^2}{c_D^4}+\frac{1}{c_S^2})s^2+O(s^3).\end{aligned} \tag{5.1}$$

Note that the second of these has no O(s^1) term, and that the O(s^1) term in the first is independent of R. Substitution of these equations into (3.6) produces

$$\vec{U}(F,P,s) = \vec{U}^0(F,P)+s\vec{U}^1(F,P)+O(s^2) \tag{5.2}$$

$$\vec{T}(F,P,s) = \vec{T}^0(F,P)+O(s^2).$$

Where the components of $\vec{U}^0$, $\vec{U}^1$, and $\vec{T}^0$ are given by

$$\begin{aligned}
U^0_{ij} &= \frac{1}{8\pi\mu(1-\nu)R}[(3-4\nu)\delta_{ij} + R_{,i}R_{,j}] \\
U^1_{ij} &= -\frac{1}{12\pi\mu(1-\nu)}\left[\frac{1-2\nu}{2c_D} + \frac{2(1-\nu)}{c_S}\right]\delta_{ij} \qquad (5.3) \\
T^0_{ij} &= -\frac{1}{8\pi(1-\nu)R^2}\left\{\frac{dR}{dn}[(1-2\nu)\delta_{ij} + 3R_{,i}R_{,j}] - (1-2\nu)(R_{,i}n_j - R_{,j}n_i)\right\}
\end{aligned}$$

With these relations, we can now form the late-time approximations for the whole–space.

5.1.1 First-Order Late-Time Approximation: LTA$^w_1$.

Let us introduce (5.2) into (3.5) and retain terms only of O(s^0). Transformation back into the time domain then yields the quasi-static relation

$$\frac{1}{2}\vec{u}(F,t) + \int_S \vec{u}(P,t)\vec{T}^0(F,P)dS_P = \int_S \vec{t}(P,t)\vec{U}^0(F,P)dS_P, \qquad (5.4)$$

which we recognize as the standard Somigliana identity for elastostatics. The relation (5.4) is based on the Green's function for an infinite elastic medium obtained by Kelvin in 1848 (Thomson, 1948). With the spatial–operator definitions

$$\begin{aligned}
\tilde{B}\vec{q}(P,t) &\equiv \int_S \vec{q}(P,t)\vec{U}^0(F,P)dS_P \\
& \qquad\qquad\qquad\qquad\qquad\qquad (5.5) \\
\tilde{\Gamma}\vec{q}(P,t) &\equiv \int_S \vec{q}(P,t)[\delta(F-P) + \vec{T}^0(F,P)]dS_P,
\end{aligned}$$

where $\delta(F-P)$ is the Dirac delta–function and $\tilde{}$ denotes a spatial tensor-integral operator, (5.4) may be expressed as LTA$^w_1$:

$$\vec{t}(P,t) = \tilde{B}^{-1}\tilde{\Gamma}\vec{u}(F,t). \qquad (5.6)$$

LTA_1^W is a *spatialy non-local, singly asymptotic, quasi–static* approximation.

5.1.2 Second-Order Late-Time Approximation: LTA_2^w.

Now we introduce (5.2) into (3.5) and retain terms through $\mathrm{O}(s^1)$. This yields

$$\frac{1}{2}\vec{u}(F,s) + \int_S \vec{u}(P,s)\vec{T}^0(F,P)dS_P = \int_S \vec{t}(P,s)\vec{U}^0(F,P)dS_P + s\int_S \vec{t}(P,s)\vec{U}^1(F,P)dS_P. \tag{5.7}$$

With the spatial–operator definitions (5.5) and the new spatial–operator

$$\tilde{A}\vec{q}(P,t) \equiv \int_S \vec{q}(P,t)\vec{U}^1(F,P)dS_P. \tag{5.8}$$

(5.7) may be expressed as the low-frequency approximation LFA_2^w:

$$(s\tilde{A} + \tilde{B})\vec{t}(P,s) = \tilde{\Gamma}\vec{u}(F,s). \tag{5.9}$$

Transformation of this equation back into the time domain produces the second-order Late-Time Approximation for the whole space LTA_2^w:.

$$\tilde{A}\dot{\vec{t}}(P,t) + \tilde{B}\vec{t}(P,t) = \tilde{\Gamma}\vec{u}(F,t) \tag{5.10}$$

LTA_2^W is a *spatialy non-local, singly asymptotic* approximation.

5.2 LATE-TIME APPROXIMATIONS FOR A HALF–SPACE.

In this section we derive the late-time approximations for a semi-infinite domain, or half–space. We will use the same method as that used in the previous section for the whole–space.

Only the A, B, C, P, Q, and S coefficients given in the appendix are dependent on s. We need to expand these coefficients in Taylor series about $s = 0$ to find the first- and second-order late-time approximations. The expansions for the unique terms are:

$$
\begin{aligned}
A_1 &= \left(\frac{1}{2\,R_1} + \frac{c_S{}^2}{2\,c_D{}^2\,R_1}\right) + \left(\frac{-2}{3\,c_S} - \frac{c_S{}^2}{3\,c_D{}^3}\right)\,s + \left(\frac{3\,R_1}{8\,c_S{}^2} + \frac{c_S{}^2\,R_1}{8\,c_D{}^4}\right)\,s^2 \\
&+ \mathrm{O}(s^3) \\
B_1 &= \left(\frac{-1}{2\,R_1} + \frac{c_S{}^2}{2\,c_D{}^2\,R_1}\right) + \left(\frac{R_1}{8\,c_S{}^2} - \frac{c_S{}^2\,R_1}{8\,c_D{}^4}\right)\,s^2 + \mathrm{O}(s^3) \\
A_3 &= \left(\frac{-3}{2\,R_2{}^2} + \frac{3\,c_S{}^2}{2\,c_D{}^2\,R_2{}^2}\right) + \left(\frac{1}{8\,c_S{}^2} - \frac{c_S{}^2}{8\,c_D{}^4}\right)\,s^2 + \mathrm{O}(s^3) \\
B_3 &= \left(\frac{-1}{2\,R_2{}^2} + \frac{c_S{}^2}{2\,c_D{}^2\,R_2{}^2}\right) + \left(\frac{1}{8\,c_S{}^2} - \frac{c_S{}^2}{8\,c_D{}^4}\right)\,s^2 + \mathrm{O}(s^3) \\
C_3 &= \left(\frac{-1}{2\,R_2{}^2} + \frac{3\,c_S{}^2}{2\,c_D{}^2\,R_2{}^2}\right) + \left(\frac{-1}{8\,c_S{}^2} - \frac{3\,c_S{}^2}{8\,c_D{}^4}\right)\,s^2 + \mathrm{O}(s^3) \qquad (5.11) \\
B_4 &= \left(\frac{-1}{2\,R_2{}^2} - \frac{c_S{}^2}{2\,c_D{}^2\,R_2{}^2}\right) + \left(\frac{1}{8\,c_S{}^2} + \frac{3\,c_S{}^2}{8\,c_D{}^4}\right)\,s^2 + \mathrm{O}(s^3) \\
A_6 &= \left(\frac{3}{2\,R_2{}^3} + \frac{3\,c_S{}^2}{2\,c_D{}^2\,R_2{}^3}\right) + \left(\frac{-1}{8\,c_S{}^2\,R_2} - \frac{3\,c_S{}^2}{8\,c_D{}^4\,R_2}\right)\,s^2 + \mathrm{O}(s^3) \\
B_6 &= \left(\frac{-1}{2\,R_2{}^3} - \frac{c_S{}^2}{2\,c_D{}^2\,R_2{}^3}\right) + \left(\frac{1}{8\,c_S{}^2\,R_2} + \frac{3\,c_S{}^2}{8\,c_D{}^4\,R_2}\right)\,s^2 + \mathrm{O}(s^3) \\
S_3 &= \left(\frac{1}{2\,R_2{}^2} + \frac{c_S{}^2}{2\,c_D{}^2\,R_2{}^2}\right) + \left(\frac{-3}{8\,c_S{}^2} - \frac{c_S{}^2}{8\,c_D{}^4}\right)\,s^2 + \mathrm{O}(s^3)
\end{aligned}
$$

The terms of $\mathrm{O}(s^0)$ are those that produce the first-order LTA for an elastic half–space. The expression for A_1 contains the only $\mathrm{O}(s^1)$ term. Thus, only U^1_{zz}, U^2_{zz}, U^1_{xx}, and U^2_{xx} contribute to the second-order LTA. We note that the tensor operator $\vec{T}(F,P)$ involves spatial deriviatives of the components of $\vec{U}$ (Brebbia and others, 1984), (Cruse and Rizzo, 1968). Additionally, the expression for A_1 is independent of position (no R dependency). Therefore, $\vec{T}(F,P)$ will contribute only $\mathrm{O}(s^0)$ terms to the second-order LTA, as is the case for the whole-space formulation.

5.2.1 First-Order Late-Time Approximation: LTA_1^H.

The first–order LTA for a half-space is a quasi–static approximation expressed by (5.4), but with $\vec{T}^0(F,P)$ and $\vec{U}^0(F,P)$ given by expressions corresponding to the half–space Green's function of Mindlin (Mindlin, 1936), rather than that of Kelvin (Brebbia and others, 1984). These expressions are constructed by augmenting (5.3), the Kelvin solution, with additional terms (Brebbia and others, 1984). The additional terms, for both the $\vec{U}^0(F,P)$ and $\vec{T}^0(F,P)$, are the $\mathrm{O}(s^0)$ terms of U^2 through U^6, [see (A.1), (A.2)].

For $\vec{U}_H^0(F,P)$, the augmentation is

$$\vec{U}_H^0(F,P) = \vec{U}^0(F,P) + \vec{U}^*(F,P) \tag{5.12}$$

in which the components of $\vec{U}^*(F,P)$ are;

$$
\begin{aligned}
U^*_{zz} &= K_d\left[8(1-\nu)^2-(3-4\nu)+\frac{(3-4\nu)r_1^2-2c\bar{x}}{R_2^2}+\frac{6c\bar{x}r_1^2}{r^4}\right] \\
U^*_{zx} &= K_d r_2\left[\frac{(3-4\nu)r_1}{R_2^2}-\frac{4(1-\nu)(1-2\nu)}{r+r_1}+\frac{6c\bar{x}r_1}{r^4}\right] \\
U^*_{xz} &= K_d r_2\left[\frac{(3-4\nu)r_1}{R_2^2}+\frac{4(1-\nu)(1-2\nu)}{r+r_1}-\frac{6c\bar{x}r_1}{r^4}\right] \\
U^*_{xx} &= K_d\left[1+\frac{(3-4\nu)r_2^2}{R_2^2}+\frac{2c\bar{x}}{R_2^2}\left(\frac{1-3r_2^2}{R_2^2}\right)\right. \\
&\qquad \left.+\frac{4r(1-\nu)(1-2\nu)}{r+r_1}\left(1-\frac{r_2^2}{R_2(r+r_1)}\right)\right] \qquad (5.13) \\
U^*_{xy} &= K_d r_2 r_3\left[\frac{(3-4\nu)}{R_2^2}-\frac{4(1-\nu)(1-2\nu)}{R_2(r+r_1)^2}-\frac{6c\bar{x}}{r^4}\right] \\
U^*_{zy} &= \frac{r_3 U^*_{zx}}{r_2} \\
U^*_{yz} &= \frac{r_3 U^*_{zy}}{r_2} \\
U^*_{yx} &= U^*_{xy} \\
U^*_{yy} &= K_d\left[1+\frac{(3-4\nu)r_3^2}{R_2^2}+\frac{2c\bar{x}}{R_2^2}\left(1-\frac{3r_3^2}{R_2^2}\right)\right. \\
&\qquad \left.+\frac{4r(1-\nu)(1-2\nu)}{r+r_1}\left(1-\frac{r_3^2}{R_2(r+r_1)}\right)\right]
\end{aligned}
$$

where $K_d = \frac{1}{16\pi(1-\nu)\mu r}$ and (see Figure 5-1)

$$r_1 = z(F)-z(P) \quad r_2 = x(F)-x(P) \quad r_3 = y(F)-y(P)$$

$$r_1' = z(F)-z(P') \quad r_2' = x(F)-x(P') \quad r_3' = y(F)-u(P')$$

$$R = (r_i r_i)^{\frac{1}{2}} \qquad R_2 = (r_i' r_i')^{\frac{1}{2}}$$

$$\bar{x} = z(F) \qquad c = z(P)$$

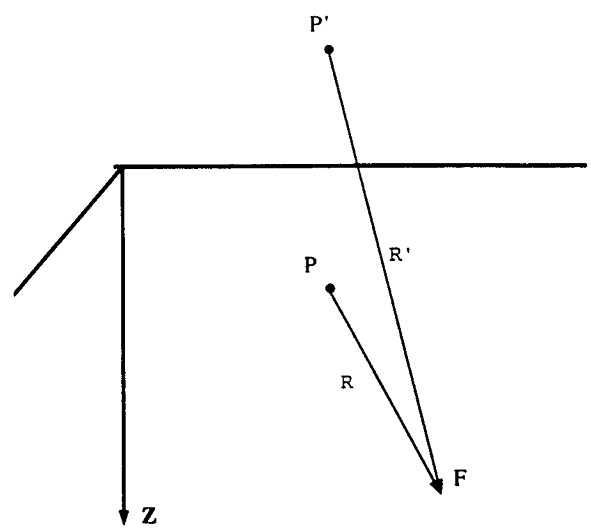

Figure 5-1. Three-dimensional geometry (in case of the half–space, the infinite free surface lies in the x - y plane).

$\vec{T}(F, P)$ is augmented as

$$\vec{T}_H(F, P) \quad = \quad \vec{T}(F, P) + \vec{T}^*(F, P) \tag{5.14}$$

in which the components of $\vec{T}^*(F, P)$ are given by

$$T^*_{ij} = \sigma^*_{jki} n_k \qquad\qquad z = 1,\ x = 2,\ y = 3 \tag{5.15}$$

where n_k is the surface normal (defined as positive going *into* the medium), and where the components of σ^* are, with $K_t = \frac{1}{8\pi(1-\nu)}$,

$$\sigma^*_{zzz} = \frac{K_t}{R_2^3}\left[1 - 2\nu r_1 - \frac{3(3-4\nu)\bar{x}r_1'^2 - 3cr_1'(5\bar{x}-c)}{R_2^2} - \frac{30c\bar{x}r_1'^3}{R_2^4}\right]$$

$$\sigma^*_{zxz} = \frac{K_t r_2}{R_2^3}\left[1 - 2\nu - \frac{3(3-4\nu)\bar{x}r_1' - 9c\bar{x} - 3c^2}{R_2^2} - \frac{30c\bar{x}r_1'^2}{R_2^4}\right]$$

$$\sigma^*_{zyz} = \frac{K_t r_3}{R_2^3}\left[1 - 2\nu - \frac{3(3-4\nu)\bar{x}r_1' - 9c\bar{x} - 3c^2}{R_2^2} - \frac{30c\bar{x}r_1'^2}{R_2^4}\right]$$

$$\begin{aligned}\sigma^*_{xxz} = \frac{K_t}{R_2^3}\Bigg[&(1-2\nu)(3r_1 - 4\nu r_1') - \frac{3(3-4\nu)r_1r_2^2}{R_2^2} \\ &+6cr_1'\frac{(1-2\nu\bar{x}-2\nu c)}{R_2^2} - \frac{30c\bar{x}r_2^2r_1'}{R_2^4} \\ &-\frac{4r^2(1-\nu)(1-2\nu)}{r+r_1}\left(1 - \frac{r_2^2}{R_2(r+r_1)} - \frac{r_2^2}{R_2^2}\right)\Bigg]\end{aligned}$$

$$\sigma^*_{xyz} = \frac{K_t r_2 r_3}{R_2^2}\left[-\frac{3(3-4\nu)r_1}{R_2^3} + \frac{4(1-\nu)(1-2\nu)}{r+r_1}\left(\frac{1}{r+r_1} + \frac{1}{R_2}\right) - \frac{30c\bar{x}r_1'}{R_2^5}\right]$$

$$\begin{aligned}\sigma^*_{yyz} = \frac{K_t}{R_2^3}\Bigg[&(1-2\nu)(3r_1 - 4\nu r_1') - \frac{3(3-4\nu)r_1r_3^2}{R_2^2} - \frac{6cr_1'[(1-2\nu)\bar{x} - 2\nu c]}{R_2^2} \\ &-\frac{30c\bar{x}r_3^2r_1'}{R_2^4} - \frac{4r^2(1-\nu)(1-2\nu)}{r+r_1}\left(1 - \frac{r_3^2}{R_2(r+r_1)} - \frac{r_3^2}{R_2^2}\right)\Bigg]\end{aligned}$$

$$\sigma^*_{zzx} = \frac{K_t r_2}{R_2^3}\left[-(1-2\nu) - \frac{3(3-4\nu)r_1^2}{R_2^2} + \frac{6c}{R_2^2}\left(c + (1-2\nu)r_1' + \frac{5\bar{x}r_1'^2}{R_2^2}\right)\right] \tag{5.16}$$

$$\sigma^*_{zxx} = \frac{K_t}{R_2^3}\left[(1-2\nu)r_1 - \frac{3(3-4\nu)r_2^2r_1'}{R_2^2} - \frac{6c}{R_2^2}\left(\bar{x}r_1' - (1-2\nu)r_2^2 - \frac{5\bar{x}r_2^2r_1'}{R_2^2}\right)\right]$$

$$\sigma^*_{zyx} = \frac{K_t r_2 r_3}{R_2^5}\left[-3(3-4\nu)r_1' + 6c\left(1 - 2\nu + \frac{5\bar{x}r_1'}{R_2^2}\right)\right]$$

$$\begin{aligned}\sigma^*_{xxx} = \frac{K_t r_2}{R_2^3}\Bigg[&(1-2\nu)(5-4\nu) - \frac{3(3-4\nu)r_2^2}{R_2^2} - \frac{4r^2(1-\nu)(1-2\nu)}{(r+r_1)^2} \\ &\left(3 - \frac{r_2^2(3R_2 + r_1')}{R_2^2(r+r_1)}\right) \\ &+\frac{6c}{R_2^2}\left(3c - 3 - 2\nu r_1' + \frac{5\bar{x}}{r^2}r_2^2\right)\Bigg]\end{aligned}$$

$$
\begin{aligned}
\sigma^*_{xyx} &= \frac{K_t r_3}{R_2^3}\left[1-2\nu-\frac{3(3-4\nu)r_2^2}{R_2^2}-\frac{4r^2(1-\nu)(1-2\nu)}{(r+r_1)^2}\left(1-\frac{r_2^2(3R_2+r_1')}{R_2^2(r+r_1)}\right)\right.\\
&\left.-\frac{6c\bar{x}}{R_2^2}\left(1-\frac{5r_2^2}{R_2^2}\right)\right]\\
\sigma^*_{yyx} &= \frac{K_t r_2}{R_2^3}\left[(1-2\nu)(3-4\nu)-\frac{3(3-4\nu)r_3^2}{R_2^2}\right.\\
&-\frac{4r^2(1-\nu)(1-2\nu)}{(r+r_1)^2}\left(1-\frac{r_3^2(3R_2+r_1')}{R_2^2(r+r_1)}\right)\\
&\left.+\frac{6c}{R_2^2}\left(c-(1-2\nu)r_1'+\frac{5\bar{x}}{r^2}r_3^2\right)\right]\\
\sigma^*_{zzy} &= \sigma^*_{112}\frac{r_3}{r_2}\\
\sigma^*_{zxy} &= \sigma^*_{132}\\
\sigma^*_{zyy} &= \frac{K_t}{R_2^3}\left[(1-2\nu)r_1-\frac{3(3-4\nu)r_3^2 r_1'}{R_2^2}-\frac{6c}{R_2^2}\left(\bar{x}r_1'-(1-2\nu)r_3^2-\frac{5\bar{x}r_3^2 r_1'}{R_2^2}\right)\right]\\
\sigma^*_{xxy} &= \frac{K_t r_3}{R_2^3}\left[(1-2\nu)(3-4\nu)-\frac{3(3-4\nu)r_2^2}{R_2^2}\right.\\
&-\frac{4r^2(1-\nu)(1-2\nu)}{(r+r_1)^2}\left(1-\frac{r_2^2(3R_2+r_1')}{R_2^2(r+r_1)}\right)\\
&\left.+\frac{6c}{R_2^2}\left(c-(1-2\nu)r_1'+\frac{5\bar{x}}{r^2}r_2^2\right)\right]\\
\sigma^*_{xyy} &= \frac{K_t r_2}{R_2^3}\left[1-2\nu-\frac{3(3-4\nu)r_3^2}{R_2^2}-\frac{4r^2(1-\nu)(1-2\nu)}{(r+r_1)^2}\left(1-\frac{r_3^2(3R_2+r_1')}{R_2^2(r+r_1)}\right)\right.\\
&\left.-\frac{6c\bar{x}}{R_2^2}\left(1-\frac{5r_3^2}{R_2^2}\right)\right]\\
\sigma^*_{yyy} &= \frac{K_t r_3}{R_2^3}\left[(1-2\nu)(5-4\nu)-\frac{3(3-4\nu)r_3^2}{R_2^2}-\frac{4r^2(1-\nu)(1-2\nu)}{(r+r_1)^2}\left(3-\frac{r_3^2(3R_2+r_1')}{R_2^2(r+r_1)}\right)\right.\\
&\left.+\frac{6c}{R_2^2}\left(3c-(3-2\nu)r_1'+\frac{5\bar{x}}{r^2}r_3^2\right)\right].
\end{aligned}
$$

In operator notation, LTA_1 for the semi–infinite domain appears the same as that for the infinite domain, given by (5.6).

5.2.2 Second-Order Late-Time Approximation: LTA_2^H.

The second-order late-time approximation includes both $O(s^0)$ and $O(s^1)$ terms in the half-space operators. In (A.1) and (A.2), the U^1 components pertain to the Kelvin solution. The U^2 components, which are the image complements to U^1, contribute components that have $O(s^1)$ terms. From the discussion following (5.11), there are no $O(s^1)$ components of the $\vec{T}$ operator. Thus, the operators for the second-order approximation are [c.f., (5.2)]

$$\begin{aligned} \vec{U}_H(F,P) &= \vec{U}_H^0(F,P) + \vec{U}_H^1(F,P) + O(s^2) \\ \vec{T}_H(F,P) &= \vec{T}_H^0(F,P) + O(s)^2. \end{aligned} \tag{5.17}$$

When we substitute the results of (5.17) into (3.5), we get

$$\frac{1}{2}\vec{u}(F,s) + \int_S \vec{u}(P,s)\vec{T}_H^0(F,P)dS_P = \int_S \vec{t}(P,s)\vec{U}_H^0(F,P)dS_P + s\int_S \vec{t}(P,s)\vec{U}_H^1(F,P)dS_P \tag{5.18}$$

We can express this equation using the spatial-operators definitiions of (5.5) and (5.8) as the second-order low-frequency approximation for a half–space

$$LFA_2^H: \qquad [s\tilde{A} + \tilde{B}]\vec{t}(P,s) = \tilde{\Gamma}\vec{u}(F,s). \tag{5.19}$$

Inverse-transforming to the time domain we obtain the second-order late-time approximation for the half–space.

$$LTA_2^H: \qquad \tilde{A}\dot{\vec{t}}(P,t) + \tilde{B}\vec{t}(P,t) = \tilde{\Gamma}\vec{u}(F,s). \tag{5.20}$$

We have now completed the formulation of both the first-order and second-order late-time approximations for the half–space. A notable result is that the late-time approximations for the half–space have the same forms as their counterparts for the whole–space.

SECTION 6

DOUBLY ASYMPTOTIC APPROXIMATIONS

In this chapter we combine, in systematic fashion, the early-time and late-time approximations into first-order and second-order doubly asymptotic approximations for both whole- and half-spaces. We conclude with the discretization of the DAA relationships using the boundary element method.

6.1 FIRST-ORDER DOUBLY ASYMPTOTIC APPROXIMATIONS.

Because the only differences between the first–order early– and late–time approximations for infinite and semi–infinite domains reside in the operators $\vec{T}(F,P)$ and $\vec{U}(F,P)$, we can formally develop first–order DAA's for the two domains simultaneously. We use the method of operator matching for this purpose (Nicholas-Vullierme, 1991), (Geers and Zhang, 1991). The appropriate trial equation is

$$\vec{t}(P,s) = [s\tilde{U}_1 + \tilde{U}_0]\vec{u}(F,s) \tag{6.1}$$

where the unkown spatial operators $\tilde{U}_0$ and $\tilde{U}_1$ are not functions of s.

For s$\rightarrow$ 0, we write (6.1) as

$$\vec{t}(P,s) = [\tilde{U}_0 + \mathrm{O}(s)]\vec{u}(F,s) \tag{6.2}$$

and match with (5.6) as s$\rightarrow$ 0, which yields

$$\tilde{U}_0 = \tilde{B}^{-1}\tilde{\Gamma}. \tag{6.3}$$

This is the asymptotic match for the static limit.

For s$\rightarrow \infty$, we write (6.1) as

$$\vec{t}(P,s) = [\tilde{U}_1 + \mathrm{O}(s^{-1})]s\vec{u}(F,s) \tag{6.4}$$

and match with (4.41) as s$\rightarrow \infty$ to get

$$\tilde{U}_1 = \rho\vec{C}. \tag{6.5}$$

Introducing this result and (6.3) into (6.1), we obtain, in transform space,

$$DAA_1(s): \qquad \vec{t}(P,s) = \left[\rho\vec{C}s + \tilde{B}^{-1}\tilde{\Gamma}\right]\vec{u}(F,s) \tag{6.6}$$

and in the time domain

$$DAA_1(t): \qquad \vec{t}(P,t) = \rho\vec{C}\dot{\vec{u}}(F,t) + \tilde{B}^{-1}\tilde{\Gamma}\vec{u}(F,t) \tag{6.7}$$

This result was heuristically formulated by Underwood and Geers (Underwood and Geers, 1981). Note that the DAA_1 for elastic domains is not spatially local, because of the second term on the right, which is the result of $s \rightarrow 0$ matching.

6.2 SECOND-ORDER DOUBLY ASYMPTOTIC APPROXIMATIONS.

In this section we develop second-order DAA's consisting of a two-term low-frequency component and a two-term high-frequency component. For the reason given in the previous section, we can develop the whole-space and half-space DAA's simultaneously.. The appropriate trial equation is

$$(s+\tilde{T}_0)\vec{t}(P,s) = (s^2\rho\vec{C} + s\tilde{U}_1 + \tilde{U}_0)\vec{u}(F,s)$$

in which highest-frequency matching has already been performed, and $\tilde{T}_0$, $\tilde{U}_1$, and $\tilde{U}_0$ are unknown spatial operators that are not functions of s.

We first match the trial equation as $s \to 0$ with the low frequency approximations (5.9) and (5.19). The left side of these may be inverted to yield

$$\vec{t}(P,s) = [I - s\tilde{B}^{-1}\tilde{A} + O(s^2)]\tilde{B}^{-1}\tilde{\Gamma}\vec{u}(F,s), \tag{6.8}$$

inasmuch as $(\tilde{B}+s\tilde{A})^{-1} = (I+s\tilde{B}^{-1}\tilde{A})^{-1}\tilde{B}^{-1} = [I - s\tilde{B}^{-1}\tilde{A} + O(s^2)]\tilde{B}^{-1}$. Similarly, the left side of (6.8) may be inverted to obtain

$$\vec{t}(P,s) = [I - s\tilde{T}_0^{-1} + O(s^2)]\tilde{T}_0^{-1}(\tilde{U}_0 + s\tilde{U}_1 + s^2\rho\vec{C})\vec{u}(F,s). \tag{6.9}$$

We can first match (6.8) and (6.9) to $O(s^0)$ to obtain

$$\tilde{T}_0^{-1}\tilde{U}_0 = \tilde{B}^{-1}\tilde{\Gamma}. \tag{6.10}$$

and then match to $O(s^1)$ to get

$$\tilde{T}_0^{-1}(\tilde{U}_1 - \tilde{T}_0^{-1}\tilde{U}_0) = -\tilde{B}^{-1}\tilde{A}\tilde{B}^{-1}\tilde{\Gamma}. \tag{6.11}$$

We now match the trial equation as $s \to \infty$ to the second-order high-frequency approximation, (4.43), which we write as

$$[\mathbf{I} + s^{-1}\kappa\vec{C}]\vec{t}(F,s) = (\rho\vec{C} + s^{-1}\kappa\vec{\Lambda})s\vec{u}(F,s) \tag{6.12}$$

Note that we have already matched at $O(s^0)$. To match at $O(s^{-1})$, we divide (6.8) through by s^1 to get

$$(\mathbf{I} + s^{-1}\tilde{T}_0)\vec{t}(P,s) = (\rho\vec{C} + s^{-1}\tilde{U}_1 + s^{-2}\tilde{U}_0)s\vec{u}(P,s) \tag{6.13}$$

The left sides of (6.12) and (6.13) may be inverted as $s \to \infty$ to get

$$\begin{aligned}\vec{t}(F,s) &= [I - s^{-1}\kappa\vec{C} + O(s^{-2})][\rho\vec{C} + s^{-1}\kappa\vec{\Lambda}]s\vec{u}(F,s)\\ \vec{t}(F,s) &= [I - s^{-1}\tilde{T}_0 + O(s^{-2})][\rho\vec{C} + s^{-1}\tilde{U}_1 + O(s^{-2})]s\vec{u}(F,s)\end{aligned} \tag{6.14}$$

Thus, matching the $\mathrm{O}(s^{-1})$ terms, we obtain

$$\tilde{U}_1 - \rho\tilde{T}_0\vec{C} = \kappa\vec{\Lambda} - \rho\kappa\vec{C}^2 \tag{6.15}$$

From (6.10), (6.11) and (6.15), the three unknown spatial operators may be found as

$$\begin{aligned}
\tilde{T}_0 &= \left[\tilde{B}^{-1}\tilde{\Gamma} + \kappa(\rho\vec{C}^2 - \vec{\Lambda})\right](\rho\vec{C} + \tilde{B}^{-1}\tilde{A}\tilde{B}^{-1}\tilde{\Gamma})^{-1} \equiv \tilde{\Omega} \\
\tilde{U}_1 &= \tilde{B}^{-1}\tilde{\Gamma} - \tilde{\Omega}\tilde{B}^{-1}\tilde{A}\tilde{B}^{-1}\tilde{\Gamma} \\
\tilde{U}_0 &= \tilde{\Omega}\tilde{B}^{-1}\tilde{\Gamma}.
\end{aligned} \tag{6.16}$$

Substitution of these results back into the trial equation produces the second-order DAA in s-space:

$$DAA_2(s): \qquad [s + \tilde{\Omega}]\vec{t} = [s^2\rho\vec{C} + s(\tilde{B}^{-1}\tilde{\Gamma} - \tilde{\Omega}\tilde{B}^{-1}\tilde{A}\tilde{B}^{-1}\tilde{\Gamma}) + \tilde{\Omega}\tilde{B}^{-1}\tilde{\Gamma}]\vec{u}. \tag{6.17}$$

Inverse transformation then yields the second-order DAA in the time domain:

$$DAA_2(t): \qquad \dot{\vec{t}} + \tilde{\Omega}\vec{t} = \rho\vec{C}\ddot{\vec{u}} + (\tilde{B}^{-1}\tilde{\Gamma} - \tilde{\Omega}\tilde{B}^{-1}\tilde{A}\tilde{B}^{-1}\tilde{\Gamma})\dot{\vec{u}} + \tilde{\Omega}\tilde{B}^{-1}\tilde{\Gamma}\vec{u}. \tag{6.18}$$

6.3 MIXED-ORDER DAA.

Here, a one-term low-frequency matching is combined with a two-term high-frequency matching to form the mixed doubly asymptotic approximation DAA_{1-2}.

The trial equation is again (6.8). For the low-frequency match we use (5.9) with $\tilde{A} = 0$. The matching procedure of the previous section then yields (6.16) with $\tilde{A} = 0$. Thus we obtain the mixed-order DAA

$$DAA_{1-2}(s): \qquad [s + \tilde{\Omega}_{1-2}]\vec{t} = [s^2\rho\vec{C} + s\tilde{B}^{-1}\tilde{\Gamma} + \tilde{\Omega}_{1-2}\tilde{B}^{-1}\tilde{\Gamma}]\vec{u}, \tag{6.19}$$

$$DAA_{1-2}(t): \qquad \dot{\vec{t}} + \tilde{\Omega}_{1-2}\vec{t} = \rho\vec{C}\ddot{\vec{u}}(t) + \tilde{B}^{-1}\tilde{\Gamma}\dot{\vec{u}}(t) + \tilde{\Omega}_{1-2}\tilde{B}^{-1}\tilde{\Gamma}\vec{u}(t). \tag{6.20}$$

where $\tilde{\Omega}_{1-2} = \left[\rho^{-1}\tilde{B}^{-1}\tilde{\Gamma}\vec{C}^{-1} + \kappa(\vec{C} - \rho^{-1}\vec{\Lambda}\vec{C}^{-1})\right]$.

6.4 BOUNDARY ELEMENT DISCRETIZATION.

A robust method for applying DAA's to general surfaces is finite element discretization methods (Underwood and Geers, 1981), (Mathews and Geers, 1987). We will discretize the ETA_2 first, by invoking the Bubnov-Galerkin
method (Cook *et al.*, 1989). We have, then

$$\begin{aligned}
\vec{u}(F,t) &= \mathbf{N}(F)\mathbf{u}(t) \\
\vec{t}(F,t) &= \mathbf{N}(F)\mathbf{t}(t).
\end{aligned} \tag{6.21}$$

where a boldface quantity denotes a computational (n-dimensional) vector or matrix. In (6.21), $\mathbf{u}(t)$ is the vector for nodal displacements of the entire discretized surface, $\mathbf{t}(t)$ is the corresponding vector of nodal tractions, and $\mathrm{N}(F)$ is a matrix of shape functions that interpolate nodal values from the nodes to the point F. Applying Bubnov-Galerkin discretization to (4.42), we obtain the matrix ETA$_2$

$$\dot{\mathbf{t}}(t) + \mathbf{F}\mathbf{t}(t) = \mathbf{D}\ddot{\mathbf{u}}(t) + \mathbf{L}\dot{\mathbf{u}}(t), \tag{6.22}$$

where

$$\mathbf{F} = \int \mathrm{N}^T(F)\kappa\vec{C}\mathrm{N}(F)\,dS$$
$$\mathbf{D} = \int \mathrm{N}^T(F)\rho\vec{C}\mathrm{N}(F)\,dS$$
$$\mathbf{L} = \int \mathrm{N}^T(F)\kappa\vec{\Lambda}\mathrm{N}(F)\,dS,$$

Similarly, the matrix ETA$_1$ follows from (4.40) as

$$\mathbf{t}(t) = \mathbf{D}\dot{\mathbf{u}}(t). \tag{6.23}$$

Discretization of the late-time approximations proceeds in the same way, so that (5.10) yields the matrix LTA$_2$

$$\mathbf{A}\dot{\mathbf{t}}(t) + \mathbf{B}\mathbf{t}(t) = \mathbf{G}\mathbf{u}(t) \tag{6.24}$$

where $\mathbf{A}$, $\mathbf{B}$, and $\mathbf{G}$ are the discretized forms of (5.8) and (5.5). The matix LTA$_1$ is obtained by taking $\mathbf{A} = 0$ in this equation.

Matrix doubly asymptotic approximations may be obtained from (6.22), (6.23), and (6.24) by the method of matrix matching, which proceeds in exactly the manner as that described in Chapter 6 for operator matching. The resulting matrix DAA$_2$ is

$$\dot{\mathbf{t}}(t) + \mathbf{W}\mathbf{t}(t) = \mathbf{D}\ddot{\mathbf{u}}(t) + (\mathbf{B}^{-1}\mathbf{G} - \mathbf{W}\mathbf{B}^{-1}\mathbf{A}\mathbf{B}^{-1}\mathbf{G})\dot{\mathbf{u}}(t) + \mathbf{W}\mathbf{B}^{-1}\mathbf{G}\mathbf{u}(t), \tag{6.25}$$

where

$$\mathbf{W} = \left[\mathbf{B}^{-1}\mathbf{G} - \mathbf{F}\mathbf{D} - \mathbf{L}\right]\left[\mathbf{D} + \mathbf{B}^{-1}\mathbf{A}\mathbf{B}^{-1}\mathbf{G}\right]^{-1},$$

The DAA$_{1-2}$ is found from (6.25) by setting the matrix operator $\mathbf{A}$ to zero. The DAA$_1$ is found by matching only the $\mathrm{O}(s^0)$ terms, it is

$$\mathbf{t}(t) = \mathbf{D}\dot{\mathbf{u}}(t) + \mathbf{B}^{-1}\mathbf{G}\mathbf{u}(t) \tag{6.26}$$

Note that we can premultiply the nodal traction vector $\mathbf{t}(t)$ by the diagonal surface-area matrix containing element areas to get the nodal force vector.

In this section we derived the DAA$_1$, DAA$_2$, and mixed-order DAA$_{1-2}$ matrix formulations used on the operator matching methods presented in section 6.2. The matrix formulations pertain to both the whole–space and half–space. The first-order matrix DAA is a first-order ordinary differential equation; the second-order DAA and the mixed-order DAA are second-order ordinary differential equations.

SECTION 7

MODAL SOLUTIONS FOR AN ELASTIC WHOLE–SPACE

In this section we develop exact $n = 0$ and $n = 1$ modal temporal impedance relations for a spherical cavity in an elastic whole–space and the corresponding DAA_2 relations. We show that the second-order modal DAA agrees with the exact temporal impedance relation for $n = 0$.

7.1 EXACT MODAL EQUATIONS FOR n =0.

This first modal derivation is based on the acoustic work of Geers and Zhang 1991 (Geers and Zhang, 1991). We start with a spherical surface in an elastic whole–space and assume motion in the radial direction only. The following equations apply:

$$\begin{aligned} u_0 &= \frac{\partial \phi_0}{\partial r} \\ \sigma_0 &= (\lambda + 2\mu)\frac{\partial^2 \phi_0}{\partial r^2} + \frac{2\lambda}{r}\frac{\partial \phi_0}{\partial r} \\ \frac{\ddot{\phi}_0}{c_D^2} &= \frac{\partial^2 \phi_0}{\partial r^2} + \frac{2}{r}\frac{\partial \phi_0}{\partial r}. \end{aligned} \tag{7.1}$$

Here, ϕ_0 is the scalar displacement potential for the $n = 0$ mode, u_0 and σ_0 represent the radial displacement and normal traction, respectively.

Laplace transforming the third of (7.1) and multiplying through by r^2, we obtain

$$r^2\frac{\partial^2 \phi_0}{\partial r^2} + 2r\frac{\partial \phi_0}{\partial r} - (\frac{sr}{c_D})^2\phi_0 = 0. \tag{7.2}$$

This equation is a form of Bessel's equation with $n = 0$ (Arfken, 1970); the solution is

$$\phi_0(r,s) = f_0(s)k_0(\frac{rs}{c_D}) = f_0(s)k_0(\xi), \tag{7.3}$$

where $\xi = {}^{rs}\!/\!_{c_D}$, $f_0(s)$ is an unknown function of the Laplace-transform variable, and $k(\xi)$ is the modified spherical Bessel function of the zeroth order.

Using the third of (7.1) to eliminate $\frac{\partial^2\phi_0}{\partial r^2}$ from the second of (7.1), Laplace transforming, and then introducing (7.3), we get

$$\sigma_0(r,s) = \rho s^2 f_0(s)k_0(\xi) - \frac{4\mu}{r}u_0. \tag{7.4}$$

Now

$$\frac{\partial k_0(\xi)}{\partial r} = \frac{s}{c_D}k_0'(\xi), \tag{7.5}$$

where $k_0'(\xi) \equiv \frac{\partial k_0}{\partial \xi}$; thus, (7.3) and the first of (7.1) yield

$$u_0(r,s) = f_0(s)\frac{s}{c_D}k_0'(\xi). \tag{7.6}$$

From (7.4)and (7.6), we obtain

$$\sigma_0(r,s) = [\rho c_D s\frac{k_0(\xi)}{k_0'(\xi)} - \frac{4\mu}{r}]u_0(r,s), \tag{7.7}$$

where the prime denotes a derivative with respect to ξ. But (Arfken, 1970),

$$\begin{aligned} k_0(\xi) &= \xi^{-1}e^{-\xi} \\ k_0'(\xi) &= -e^{-\xi}(\xi^{-1}+\xi^{-2}) \\ \frac{k_0(\xi)}{k_0'(\xi)} &= -\frac{1}{1+\xi^{-1}} \end{aligned} \tag{7.8}$$

so that (7.7) may be expressed as

$$(s+\frac{c_D}{r})p_0 = (\rho c_D s^2 + \frac{4\mu s}{r} + \frac{4\mu c_D}{r^2})u_0, \tag{7.9}$$

where the traction $p_0 = -\sigma_0$ and ξ has been replaced by $^{rs}/_{c_D}$. This is the exact modal impedance relation for $n=0$ motion of a spherical surface in an elastic whole–space.

Note that, at early times ($s \to \infty$), (7.9) yields

$$p_0 = \rho c_D \dot{u}_0, \tag{7.10}$$

which is the standard plane-wave temporal impedance relation (Love, 1904a). At late times ($s \to 0$), (7.9) yields

$$p_0 = \frac{4\mu}{r}, \tag{7.11}$$

which is the static solution.

We will now develop an $n=0$ modal impedance relation for shear traction and corresponding tangential displacement. Starting with a spherical surface in an elastic whole–space and assuming uniform tangential motion that is only a function of the radial spatial coordinate, the vector displacement becomes a scalar function. Therefore, the following equations apply:

$$\begin{aligned} v_0 &= \frac{\partial \psi_0}{\partial r} \\ \tau_0 &= \mu(\frac{\partial^2 \psi_0}{\partial r^2} - \frac{2}{r}\frac{\partial \psi_0}{\partial r}) \\ \frac{\ddot{\psi}_0}{c_S^2} &= \frac{\partial^2 \psi_0}{\partial r^2} + \frac{2}{r}\frac{\partial \psi_0}{\partial r}. \end{aligned} \tag{7.12}$$

where ψ_0 is the scalar displacement potential for the tangential $n = 0$ motion, and v_0 and τ_0 represent the tangential displacement and the shear stress on the surface, respectively, for the $n = 0$ mode. Laplace transforming the third equation of (7.12) and multiplying through by r^2, we obtain

$$r^2\frac{\partial^2\psi_0}{\partial r^2} + 2r\frac{\partial\psi_0}{\partial r} - (\frac{sr}{c_S})^2\psi_0 = 0. \tag{7.13}$$

This equation is a form of Bessel's equation with $n = 0$. Following the same process as that used for radial $n = 0$ motion, we obtain for tangential $n = 0$ motion

$$(s + \frac{c_S}{r})\tau_0 = [\rho c_S s^2 + \frac{2\mu s}{r} + \frac{2\mu c_S}{r^2}]v_0. \tag{7.14}$$

We have now derived the $n = 0$ modal-impedance relations for both radial and tangential motions. In the next section we show that DAA, when adapted to these one–dimensional problems, gives identical equations.

7.2 DAA$_2$ EQUATIONS FOR n=0.

We now develop a modal second-order doubly asymptotic approximation (DAA$_2^m$) for an elastic whole–space. Again, we follow the acoustic work of Geers & Zhang (Geers and Zhang, 1991), outlining the process for the radial motion case only, as the tangential case follows identical steps.

A second-order high-frequency approximation (HFA$_2$) is obtained by the introduction of the last of (7.8), into (7.7), which yields

$$\text{HFA}_2: \qquad (s + \frac{c_D}{r})p_0 = (\rho c_D s^2 + \frac{4\mu s}{r} + \frac{4\mu c_D}{r^2})u_0. \tag{7.15}$$

This equation is identical to the exact $n = 0$ modal equation because all the ray-theory assumptions are satisfied exactly for $n = 0$ motion.

The second-order low-frequency approximation (LFA$_2$) is found from the expansion of the last of (7.8) as $s \to 0$, which produces

$$\frac{k_0(\xi)}{k_0'(\xi)} = -\frac{1}{1+\xi^{-1}} = -\xi(1 - \xi + \xi^2) + \cdots. \tag{7.16}$$

When we substitute this result into (7.7) with $\xi = {}^{rs}\!/_{c_D}$, and keep terms of $O(s^1)$ and $O(s^0)$, we get

$$\text{LFA}_2: \qquad \sigma_0(r,s) = -(0s + \frac{4\mu}{r})u_0(r,s). \tag{7.17}$$

Because there are no terms of $O(s^1)$, the second-order low-frequency approximation (LFA$_2$) for the $n = 0$ modal solution is identical to the first-order low-frequency approximation.

To form the modal second-order DAA for an elastic whole–space, a trial equation is selected as

$$(s + T_0)p_0 = (\rho c_D s^2 + U_1 s + U_0)u_0, \tag{7.18}$$

where T_0, U_1, and U_0 are unknown constants that are not functions of s, and p_0 is the pressure, i.e., $\sigma_0 = -p_0$. Solving for p_0 in equation (7.18) we get

$$p_0 = (s + T_0)^{-1}(\rho c_D s^2 + U_1 s + U_0)u_0. \tag{7.19}$$

Now as $s \rightarrow 0$,

$$(s + T_0)^{-1} = T_0^{-1} - T_0^{-2}s + T_0^{-3}s^2 + \cdots . \tag{7.20}$$

Substituting this result into (7.19), keeping terms up to and including $O(s^1)$, and matching the terms with (7.17), we get

$$\begin{aligned} T_0^{-1}U_0 &= \frac{4\mu}{r} \\ U_1 - T_0^{-1}U_0 &= 0 \end{aligned} \tag{7.21}$$

To match the high frequency terms, we arrange the trial equation (7.18) for $s \rightarrow \infty$ as

$$p_0 = (1 - T_0 s^{-1} + T_0^2 s^{-2} \ldots)[\rho c_D + U_1 s^{-1} + U_0 s^{-2}]su_0. \tag{7.22}$$

A similar rearrangement of (7.15) yields

$$p_0 = (1 - \frac{c_D s^{-1}}{r} + (\frac{c_D}{r})^2 s^{-2} \ldots)[\rho c_D + \frac{4\mu}{r}s^{-1} + \frac{4\mu c_D}{r^2}s^{-2}]su_0. \tag{7.23}$$

Matching (7.22) and (7.23) through order s^{-1} we obtain

$$U_1 - \rho c_D T_0 = \frac{4\mu}{r} - \rho\frac{c_D^2}{r} \tag{7.24}$$

Simultaneous solution of (7.21) and (7.24) yields

$$\begin{aligned} T_0 &= \frac{c_D}{r} \\ U_0 &= \frac{4\mu c_D^2}{r^2} \\ U_1 &= \frac{4\mu}{r}, \end{aligned} \tag{7.25}$$

so that (7.18) gives for radial $n = 0$ motion,

DAA$_2^{n=0}$-radial $$(s + \frac{c_D}{r})p_0 = (\rho c_D s^2 + \frac{4\mu}{r}s + \frac{4\mu c_D}{r^2})u_0, \tag{7.26}$$

Note that this equation is identical to the exact equation (7.9). Proceeding in the same manner for tangential $n = 0$ motion, we find

$$\text{DAA}_2^{n=0}\text{-tangential} \qquad (s + \frac{c_S}{r})\tau_0 = (\rho c_S s^2 + \frac{2\mu}{r}s + \frac{2\mu c_S}{r^2})v_0, \tag{7.27}$$

which is identical to (7.14).

Regarding the assembly (7.26) and (7.27) as one doubly asymptotic approximation for $n = 0$ motion of a spherical surface, we conclude that $\text{DAA}_2^{n=0}$ is an exact relation.

7.3 EXACT MODAL EQUATIONS FOR n=1.

Now we will derive the $n = 1$ modal solution of a spherical cavity in an infinite elastic medium using direct transformation. We start with relationships between stresses and potentials for axisymmetric motions (Eringen and Suhubi, 1975).

$$\begin{aligned} \sigma &= \lambda\nabla^2\phi + 2\mu\left\{\frac{\partial^2\phi}{\partial r^2} + \frac{\partial}{\partial r}\left[\frac{\partial^2(r\psi)}{\partial r^2} - r\nabla^2\psi\right]\right\} \\ \tau &= \frac{\mu}{r}\left\{2\frac{\partial^2\phi}{\partial r\partial\theta} - \frac{2}{r}\frac{\partial\phi}{\partial\theta} - \frac{\partial}{\partial\theta}\left[\frac{\partial^2(r\psi)}{\partial r^2} - r\nabla^2\psi\right] + \frac{1}{r}\frac{\partial^2(r\psi)}{\partial\theta\partial r} - r\frac{\partial}{\partial r}\left[\frac{1}{r}\frac{\partial^2(r\psi)}{\partial\theta\partial r}\right]\right\}. \end{aligned} \tag{7.28}$$

The relationships between the radial and meridional displacements and the displacement potentials are:

$$\begin{aligned} u &= \frac{\partial\phi}{\partial r} - \left[\frac{\partial^2(r\psi)}{\partial r^2} - r\nabla^2\psi\right] \\ v &= \frac{1}{r}\frac{\partial\phi}{\partial\theta} - \frac{1}{r}\frac{\partial^2(r\psi)}{\partial\theta\partial r}. \end{aligned} \tag{7.29}$$

We can represent the displacement potentials for n= 1 as

$$\begin{aligned} \phi &= f_1(s)k_1(\xi)P_1(\cos\theta) \\ \psi &= g_1(s)k_1(\eta)P_1(\cos\theta), \end{aligned} \tag{7.30}$$

where $\xi = \frac{sr}{c_D}$, $\eta = \frac{sr}{c_S}$, k_1 is a modified spherical Bessel function, P_1 is Legendre polynominal and f_1 and g_1 are coefficients dependent only on the Laplace-transform variable s. Multiplying the above equations by $P_m(\cos\theta)$, integrating over the surface, and invoking the orthogonality property of Legendre functions, we get, after some rearrangement and substitution;

$$\begin{aligned} \sigma_1 &= \lambda\nabla_1^2\phi_1 + 2\mu\left\{\frac{\partial^2\phi_1}{\partial r^2} - \frac{\partial}{\partial r}\left[\frac{\partial^2(r\psi_1)}{\partial r^2} - r\nabla_1^2\psi_n\right]\right\} \\ \tau_1 &= -\frac{\mu}{r}\left\{2\frac{\partial\phi_1}{\partial r} - \frac{2}{r}\phi_1 - \left[\frac{\partial^2(r\psi_1)}{\partial r^2} - r\nabla^2\psi_1\right] + \frac{1}{r}\frac{\partial(r\psi_1)}{\partial r} - r\frac{\partial}{\partial r}\left[\frac{1}{r}\frac{\partial(r\psi_1)}{\partial r}\right]\right\}. \end{aligned} \tag{7.31}$$

where

$$\nabla_1^2 = \frac{\partial^2}{\partial r^2} + \frac{2}{r}\frac{\partial}{\partial r} - \frac{2}{r^2} \tag{7.32}$$

We can now eliminate the second-order partials by using the wave equations $\nabla_1^2\phi_1 = c_D^{-2}\ddot{\phi}_1$ and $\nabla_1^2\psi_1 = c_S^{-2}\ddot{\psi}_1$.

$$\begin{aligned} \sigma_1 &= \rho s^2\phi_1 - \frac{4\mu}{r}u_1 - \frac{4\mu}{r}v_1 \\ \tau_1 &= \rho s^2\psi_1 - \frac{2\mu}{r}v_1 - \frac{2\mu}{r}u_1, \end{aligned} \tag{7.33}$$

We can get the $n = 1$ relationships for the displacements (7.30) by employing Legendre functions and (7.32).

$$\begin{aligned} u_1 &= \frac{\partial\phi_1}{\partial r} - \frac{2}{r}\psi_1 \\ v_1 &= \frac{\partial\psi_1}{\partial r} + \frac{\psi_1}{r} - \frac{\phi_1}{r}, \end{aligned} \tag{7.34}$$

We can use (7.29) and the above equations to solve for f_1 and g_1 as

$$\begin{aligned} f_1 &= \frac{-c_D r(-c_S k_1(\eta) - r s k_1'(\eta))u_1 + 2 r c_D c_S k_1(\eta) v_1}{-2c_D c_S k_1(\eta)k_1(\xi) + r s c_S k_1(\eta)k_1'(\xi) + r^2 s^2 k_1'(\eta)k_1'(\xi)} \\ g_1 &= \frac{r c_D c_S k_1(\xi)u_1 + r^2 s c_S k_1'(\xi)v_1}{-2c_D c_s k_1(\eta)k_1(\xi) + r s c_S k_1(\eta)k_1'(\xi) + r^2 s^2 k_1'(\eta)k_1'(\xi)}. \end{aligned} \tag{7.35}$$

We can eliminate ϕ_1 and ψ_1 in (7.33) using f_1 and g_1 and (7.30). Substitution of the expansions for the modified spherical Bessel functions, given by

$$\begin{aligned} k_1(\xi) &= e^{-\xi}(\xi^{-2} + \xi^{-1}) \\ k_1'(\xi) &= e^{-\xi}(-2\xi^{-3} - 2\xi^{-2} - \xi^{-1}) \\ k_1(\eta) &= e^{-\eta}(\eta^{-2} + \eta^{-1}) \\ k_1'(\eta) &= e^{-\eta}(-2\eta^{-3} - 2\eta^{-2} - \eta^{-1}). \end{aligned}$$

yields the traction-displacement relations,

$$[\mathbf{I}s^2 + \frac{\mathbf{T}_1}{r}s + \frac{\mathbf{T}_0}{r^2}]\left\{ \begin{array}{c} \sigma_1 \\ \tau_1 \end{array} \right\} = [\rho\mathbf{C}s^3 + \frac{\mathbf{U}_2}{r}s^2 + \frac{\mathbf{U}_1}{r^2}s + \frac{\mathbf{U}_0}{r^3}]\left\{ \begin{array}{c} u_1 \\ v_1 \end{array} \right\} \tag{7.36}$$

where

$$\mathbf{T}_1 = \left\{ \begin{array}{cc} 2c_D + c_S & 0 \\ 0 & 2c_D + c_S \end{array} \right\} = (2c_D + c_S)\mathbf{I}$$

$$\mathbf{T}_0 = \left\{ \begin{array}{cc} 2c_D^2 + c_S^2 & 0 \\ 0 & 2c_D^2 + c_S^2 \end{array} \right\} = (2c_D^2 + c_S^2)\mathbf{I}$$

$$\mathbf{U}_2 = \left\{ \begin{array}{cc} 4\mu + \rho c_D^2 + \rho c_D c_S & 4\mu - 2\rho c_D c_S \\ 2\mu - \rho c_D c_S & 2\mu + \rho c_S^2 + 2\rho c_D c_S \end{array} \right\} \tag{7.37}$$

$$\mathbf{U}_1 = \left\{ \begin{array}{cc} 4\mu[2c_D + c_S] + \rho[c_D^2 c_S + c_D c_S^2] & 4\mu[2c_D + c_S] - 2\rho[c_D^2 c_S + c_D c_S^2] \\ 2\mu[2c_D + c_S] - \rho[c_D^2 c_S + c_D c_S^2] & 2\mu[2c_D + c_S] + 2\rho[c_D^2 c_S + c_D c_S^2] \end{array} \right\}$$

$$\mathbf{U}_0 = \left\{ \begin{array}{cc} 4\mu[2c_D^2 + c_S^2] + \rho[c_D^2 c_S^2] & 4\mu[2c_D^2 + c_S^2] - 2\rho[c_D^2 c_S^2] \\ 2\mu[2c_D^2 + c_S^2] - \rho[c_D^2 c_S^2] & 2\mu[2c_D^2 + c_S^2] + 2\rho[c_D^2 c_S^2] \end{array} \right\}$$

Equation 7.36 is the exact $n = 1$ modal equation. We will now derive various approximate relations for $n = 1$ motion.

7.3.1 n= 1 High-Frequency Approximations.

First, we write (7.36) as

$$[\mathbf{I} + r^{-1}\mathbf{T}_1 s^{-1} + r^{-2}\mathbf{T}_0 s^{-2}]\mathbf{t}_1 = [\rho\mathbf{C} + r^{-1}\mathbf{U}_2 s^{-1} + r^{-2}\mathbf{U}_1 s^{-2} + r^{-3}\mathbf{U}_0 s^{-3}]s\mathbf{u}_1, \tag{7.38}$$

where $\mathbf{t}_1$ and $\mathbf{u}_1$ represent the $n = 1$ traction and displacement vectors. To get $\mathrm{HFA}_2^{n=1}$, we drop terms of $\mathrm{O}(\mathrm{s}^{-2})$, and $\mathrm{O}(\mathrm{s}^{-3})$ inside both brackets; to get $\mathrm{HFA}_1^{n=1}$, we drop terms of $\mathrm{O}(\mathrm{s}^{-1})$, $\mathrm{O}(\mathrm{s}^{-2})$, and $\mathrm{O}(\mathrm{s}^{-3})$ inside both brackets. Thus we have

$$\mathrm{HFA}_2^{n=1}: \quad [\mathbf{I}s + \frac{1}{r}\mathbf{T}_1]\mathbf{t}_1 = [\rho\mathbf{C}s^2 + \frac{\mathbf{U}_2 s}{r}]\mathbf{u}_1, \tag{7.39}$$

$$\mathrm{HFA}_1^{n=1}: \quad \mathbf{t}_1 = \rho\mathbf{C}s\mathbf{u}_1 \tag{7.40}$$

7.3.2 n=1 Low-Frequency Approximations.

We premultiply (7.38) through by $r^2\mathbf{T}_0^{-1} = r^2/(2c_D^2 + c_S^2)$ to get

$$[1 + \frac{r}{c_1}s + (\frac{r}{c_0})^2 s^2]\,\mathbf{I}\,\mathbf{t}_1 = (rc_0^2)^{-1}[\mathbf{U}_0 + r\mathbf{U}_1 s + r^2\mathbf{U}_2 s^2 + r^3\rho\mathbf{C}s^3]\mathbf{u}_1 \tag{7.41}$$

where $c_0^2 = 2c_D^2 + c_S^2$ and $c_1 = 2c_D^2 + c_S^2/2c_D + c_S$. Now we divide through by $1 + \frac{r}{c_1}s + (\frac{r}{c_0})^2 s^2$ to get, through $\mathrm{O}(\mathrm{s}^1)$,

$$LFA_2^{n=1}: \quad \mathbf{t}_1 = [\mathbf{K}_1 + \mathbf{K'}_1 s]\mathbf{u}_1 \tag{7.42}$$

where, with $c_2^2 = (c_D c_S/c_0)^2$ and $c_3^2 = c_1 c_D c_S(c_D + c_S)/c_0^2$,

$$\mathbf{K}_1 = (rc_0^2)^{-1}\mathbf{U}_0 = \frac{1}{r}\begin{Bmatrix} 4\mu + \rho c_2^2 & 4\mu - 2\rho c_2^2 \\ 2\mu - \rho c_2^2 & 2\mu + 2\rho c_2^2 \end{Bmatrix} \tag{7.43}$$

$$\mathbf{K'}_1 = c_1^{-1}[c_0^{-2}c_1\mathbf{U}_1 - c_0^{-2}\mathbf{U}_0] = \rho c_1^{-1}(c_3^2 - c_2^2)\begin{Bmatrix} 1 & -2 \\ -1 & 2 \end{Bmatrix} \tag{7.44}$$

If we keep terms only through $O(s^0)$, we get the first-order low-frequency approximation

$\mathrm{LFA}_1^{n=1}$:

$$\mathbf{t}_1 = \mathbf{K}_1\mathbf{u}_1, \tag{7.45}$$

7.4 n= 1 DOUBLY ASYMPTOTIC APPROXIMATIONS.

As the form of the modal first-order approximations for low- and high-frequencies are similar to the form of the first-order low- and high- frequency general DAA (section 6.1), we can use the same process to combine (7.40) and (7.45) to get the first-order DAA for the $n = 1$ motion.

$DAA_1^{n=1}$

$$\mathbf{t}_1 = \rho\mathbf{C}\dot{\mathbf{u}}_1 + \mathbf{K}_1\mathbf{u}_1 \tag{7.46}$$

We can form a one-low, two-high DAA ($\mathrm{DAA}_{1-2}^{n=1}$) from (7.39), (7.45) and the trial equation

$$(s + \mathbf{T}_0)\mathbf{t}_1 = (s^2\rho\mathbf{C} + s\mathbf{U}_1 + \mathbf{U}_0)\mathbf{u}_1$$

Proceeding in the manner described in section 6.2, we get for the spatial operators

$$\begin{aligned} \mathbf{T}_0 &= [\frac{\rho\mathbf{C}\mathbf{T}_1}{r} - \frac{\mathbf{U}_2}{r} + \mathbf{K}_1][\rho\mathbf{C}]^{-1} = \mathbf{W}_1 \\ \mathbf{U}_1 &= \mathbf{K}_1 \\ \mathbf{U}_0 &= \mathbf{W}_1\mathbf{K}_1, \end{aligned} \tag{7.47}$$

which yields

$DAA_{1-2}^{n=1}$

$$(s + \mathbf{W}_1)\mathbf{t}_1 = (s^2\rho\mathbf{C} + s\mathbf{K}_1 + \mathbf{W}_1\mathbf{K}_1)\mathbf{u}_1 \tag{7.48}$$

For the full second-order DAA ($\mathrm{DAA}_2^{n=1}$), we again start with the trial equation (7.47) and employ (7.39) and (7.42). Using the matching procedures employed to obtain (7.21), we find from low-frequency matching

$$\begin{aligned} \mathbf{T}_0^{-1}\mathbf{U}_0 &= \mathbf{K}_1 \\ \mathbf{T}_0^{-1}\mathbf{U}_1 - \mathbf{T}_0^{-2}\mathbf{U}_0 &= \mathbf{K'}_1. \end{aligned} \tag{7.49}$$

The first equation is from the $O(s^0)$ match, and the second equation is from the $O(s^1)$ match. For high-frequency matching, we use the procedure employed to obtain (7.24) this yields

$$\mathbf{U}_1 - \mathbf{T}_0\rho\mathbf{C} = r^{-1}\mathbf{U}_2 - r^{-1}\mathbf{T}_1\rho\mathbf{C} \tag{7.50}$$

which results from the (s^{-1}) match. Finally, simultaneous solution of (7.49) and (7.50) yields

$$\begin{aligned}\mathbf{T}_0 &= [\frac{\mathbf{T}_1\rho\mathbf{C}}{r} - \frac{\mathbf{U}_2}{r} + \mathbf{K}_1][\rho\mathbf{C} - \mathbf{K}'_1]^{-1} = \mathbf{V}_1 \\ \mathbf{U}_1 &= \mathbf{V}_1\rho\mathbf{C} - \frac{\mathbf{T}_1\rho\mathbf{C}}{r} + \frac{\mathbf{U}_2}{r} \\ \mathbf{U}_0 &= \mathbf{V}_1\mathbf{K}_1.\end{aligned} \tag{7.51}$$

which yields DAA_2 for $n = 1$ motion

$$DAA_2^{n=1} \qquad (s + \mathbf{V}_1)\mathbf{t}_1 = \left[\rho\mathbf{C}s^2 + \left(\mathbf{V}_1\rho\mathbf{C} - \frac{\mathbf{T}_1\rho\mathbf{C}}{r} + \frac{\mathbf{U}_2}{r}\right)s + \mathbf{V}_1\mathbf{K}_1\right]\mathbf{u}_1 \tag{7.52}$$

In this section we have developed exact and DAA temporal impedance relations for $n = 0$ and $n = 1$ motions of a spherical surface embedded in an infinite elastic medium.

SECTION 8

CANONICAL PROBLEMS

Here we compare DAA-based and exact results for canonical problems, as done previously by Geers and Underwood (Underwood and Geers, 1981) and by Mathews and Geers (Mathews and Geers, 1987). In a recent analytical study, Oberai (Oberai, 1994) generated DAA-based response for step-wave-excited infinite-cylindrical and spherical shells embedded in infinite elastic media. His comparisons with corresponding exact results showed DAA_1 to be fairly satisfactory and DAA_2 to highly satisfactory.

We first discuss the computer programs developed to implement the DAA equations and then we compare results for four problems:

1. A spherical cavity embedded in an elastic whole–space subjected to an $n = 0$ internal step pressure.
2. A spherical cavity embedded in an elastic half–space subjected to an $n = 0$ internal step pressure.
3. A spherical cavity embedded in an elastic whole–space subjected to an $n = 1$ internal step traction.
4. A uniform step pressure applied to a portion of the surface of a half–space.

8.1 DAA COMPUTER PROGRAMS.

We developed three computer programs for computing DAA-based responses. The first program, EDAA1, implements the theory of first-order doubly asymptotic approximations for three-dimensional elastic media, both infinite and semi-infinite. The second program, EDAA1-2, implements the theory of the mixed-order (one-low, two high) doubly asymptotic approximation for three-dimensional infinite elastic media. The third program, EDAA2, implements the theory of second-order doubly asymptotic approximations for three-dimensional elastic media, again for both infinite and semi-infinite spaces. The routines for the first-order kernels, $\mathbf{U}^0$ and $\mathbf{T}^0$ (6.24), are based on software obtained from Mathews (Mathews, 1990).

Eight-node serendipity elements are used to discretize the surface (Hughes, 1987)(Figure 8-1). The

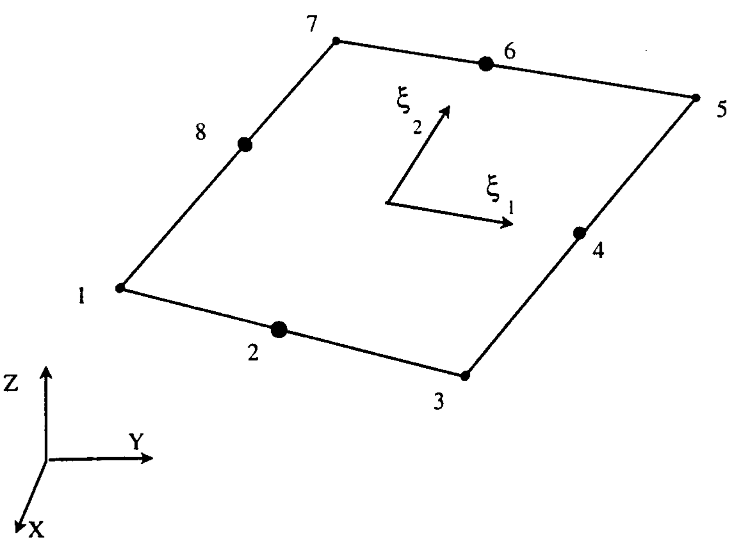

Figure 8-1. Eight node serendipity element.

weighting functions are

$$
\begin{aligned}
N_1(\xi_1,\xi_2) &= -\frac{1}{4}(1-\xi_1)(1-\xi_2)(1+\xi_1+\xi_2) \\
N_2(\xi_1,\xi_2) &= \frac{1}{2}(1-\xi_1^2)(1-\xi_2) \\
N_3(\xi_1,\xi_2) &= \frac{1}{4}(1+\xi_1)(1-\xi_2)(-1+\xi_1+\xi_2) \\
N_4(\xi_1,\xi_2) &= \frac{1}{2}(1+\xi_1)(1-\xi_2^2) \\
N_5(\xi_1,\xi_2) &= \frac{1}{4}(1+\xi_1)(1+\xi_2)(-1+\xi_1+\xi_2) \\
N_6(\xi_1,\xi_2) &= \frac{1}{2}(1-\xi_1^2)(1+\xi_2) \\
N_7(\xi_1,\xi_2) &= \frac{1}{4}(1-\xi_1)(1+\xi_2)(-1-\xi_1+\xi_2) \\
N_8(\xi_1,\xi_2) &= \frac{1}{2}(1-\xi_1)(1-\xi_2^2)
\end{aligned}
\tag{8.1}
$$

where $\xi_1 \in [-1,1]$ and $\xi_2 \in [-1,1]$. The methods explained in Section 6.4 are used to form the kernel matrices with 3×3 Gauss quadrature employed for element integration. The required matrix inversions are performed with standard Gauss elimination techniques. Due to the basic assumption of linearity, all matrices are formed only once, and decomposed once, to form the DAA equations. The loads $\mathbf{f}$ and $\dot{\mathbf{f}}$ are calculated at each step. The programs use trapezoidal time integration techniques. The first-order DAA (DAA_1) is a first-order ordinary differential equation for $\mathbf{u}$ and the mixed-order (DAA_{1-2}) and second-order DAA (DAA_2) second-order ordinary differential equation for $\mathbf{u}$. Therefore the two programs have different implementations of the trapezoidal method.

The DAA_1 (EDAA1) matrix equations (6.26) are advanced in time to step $n+1$ using the following algorithm (Hughes, 1987);

$$\begin{aligned} \tilde{\mathbf{u}}_{n+1} &= \mathbf{u}_n + \frac{\delta t}{2}\dot{\mathbf{u}}_n \\ \frac{2}{\delta t}\left(\mathbf{D} + \frac{\delta t}{2}\mathbf{B}^{-1}\mathbf{G}\right)\mathbf{u}_{n+1} &= \mathbf{f}_{n+1} + \frac{2}{\delta t}\mathbf{D}\tilde{\mathbf{u}}_{n+1} \\ \dot{\mathbf{u}}_{n+1} &= \frac{2}{\delta t}(\mathbf{u}_{n+1} - \tilde{\mathbf{u}}_{n+1}), \end{aligned} \tag{8.2}$$

where δt is the time interval used, and $\tilde{\mathbf{u}}_{n+1}$ is the predictor.

The programs EDAA1-2 and EDAA2 use the trapezoidal method for second-order differential equations. The trapezoidal method that is used for time integration in EDAA2 is shown below:

$$\begin{aligned} \left[\frac{4}{\delta t^2}\mathbf{D} + \frac{2}{\delta t}(\mathbf{B}^{-1}\mathbf{G}\right. &- \left.\mathbf{W}\mathbf{B}^{-1}\mathbf{A}\mathbf{B}^{-1}\mathbf{G}) + \mathbf{W}\mathbf{B}^{-1}\mathbf{G}\right]\mathbf{u}_{n+1} \\ &= (\mathbf{W}\mathbf{f} + \dot{\mathbf{f}}) + (\mathbf{B}^{-1}\mathbf{G} - \mathbf{W}\mathbf{B}^{-1}\mathbf{A}\mathbf{B}^{-1}\mathbf{G})(\frac{2}{\delta t}\mathbf{u}_n + \dot{\mathbf{u}}_n) \\ &+ \mathbf{D}(\frac{4}{\delta t^2}\mathbf{u}_n + \frac{4}{\delta t}\dot{\mathbf{u}}_n + \ddot{\mathbf{u}}_n) \\ \mathbf{v}_{n+1} &= \frac{2}{\delta t}(\mathbf{u}_{n+1} - \mathbf{u}_n) \\ \ddot{\mathbf{u}}_{n+1} &= \frac{2}{\delta t}\mathbf{v}_{n+1} - \frac{4}{\delta t}\dot{\mathbf{u}}_n - \ddot{\mathbf{u}}_n \\ \dot{\mathbf{u}}_{n+1} &= \mathbf{v}_{n+1} - \dot{\mathbf{u}}_n \end{aligned} \tag{8.3}$$

The time integration method for EDAA1-2 is formed from the EDAA2 by dropping terms containing $\mathbf{A}$.

8.2 SPHERICAL CAVITY/WHOLE–SPACE/STEP PRESSURE PROBLEM.

The first problem is a *spherical cavity embedded in an infinite elastic medium and excited by an internal step pressure.* This problem possesses radial symmetry, and has a well–known analytical solution (Timoshenko and Goodier, 1970). With a as the cavity radius and p_0 as the pressure magnitude, the radial displacement of the cavity is given by

$$
\begin{aligned}
u(t) \;=\; -\frac{p_0 a}{4\mu} \Big\{ & \alpha e^{-\alpha t}(\cos \alpha\beta t + \frac{1}{\beta} \sin \alpha\beta t) \\
& -\alpha e^{-\alpha t}(-\sin \alpha\beta t + \cos \alpha\beta t) \\
& +1 - e^{-\alpha t}(\cos \alpha\beta t + \frac{1}{\beta} \sin \alpha\beta t) \Big\} .
\end{aligned}
\tag{8.4}
$$

where

$$
\begin{aligned}
\alpha &= \frac{c_D(1-2\nu)}{a(1-\nu)} \\
\beta &= \sqrt{\frac{1}{1-2\nu}}
\end{aligned}
\tag{8.5}
$$

The corresponding analytical DAA_1 solution is simply

$$
u_{DAA}(t) = \frac{P_0 a}{4\mu}\left(1 - e^{-4\mu t/a\rho C_D}\right). \tag{8.6}
$$

The boundary–element model of the cavity boundary consisted of 24 eight-node elements over the entire spherical surface. The analytical exact, analytical DAA_1, and numerical DAA_1 solutions are shown in Figure 8-2 for the parameters $\rho = 1.00$, $\mu = 1/6$, $\nu = 1/4$, $a = 1$, and $p_0 = 1$. The analytical DAA_1 and numerical DAA_1 solutions are seen to be almost identical, and the DAA_1 solutions agree well with the analytical exact solution at both early and late times. As previously observed by Underwood and Geers (Underwood and Geers, 1981), the DAA_1 solutions do not exhibit the response overshoot seen in the exact solution. This is expected from first–order differential equations like (6.7).

The radial displacement response from the second–order DAA_2 (EDAA2) is compared with the exact response in Figure 8-3. Also in this figure is the DAA_1 boundary-element result. The agreement between the second-order DAA and the exact analytical solution is excellent. The small difference between the two results is due to element discretization, which yields a discrepancy in surface area of 1%. The second-order DAA_2 yields the "overshoot" characteristic of elastic media problems.

Figure 8-4 shows a comparison of exact, boundary element DAA_1, mixed-order modal DAA_{1-2}, and mixed-order boundary element DAA (EDAA12) results, for the cavity subjected to an internal step pressure. The exact Timoshenko and the modal DAA_{1-2} results are identical. This is because LTA_1 is identical to LTA_2 for this case.

8.3 SPHERICAL CAVITY/ WHOLE–SPACE/n=1 STEP TRACTIONS PROBLEM.

This problem involves a *spherical cavity embedded in an infinite elastic medium and excited by an* $n = 1$ *internal step traction.* The problem is axisymmetric. The exact modal relation, (7.36), includes

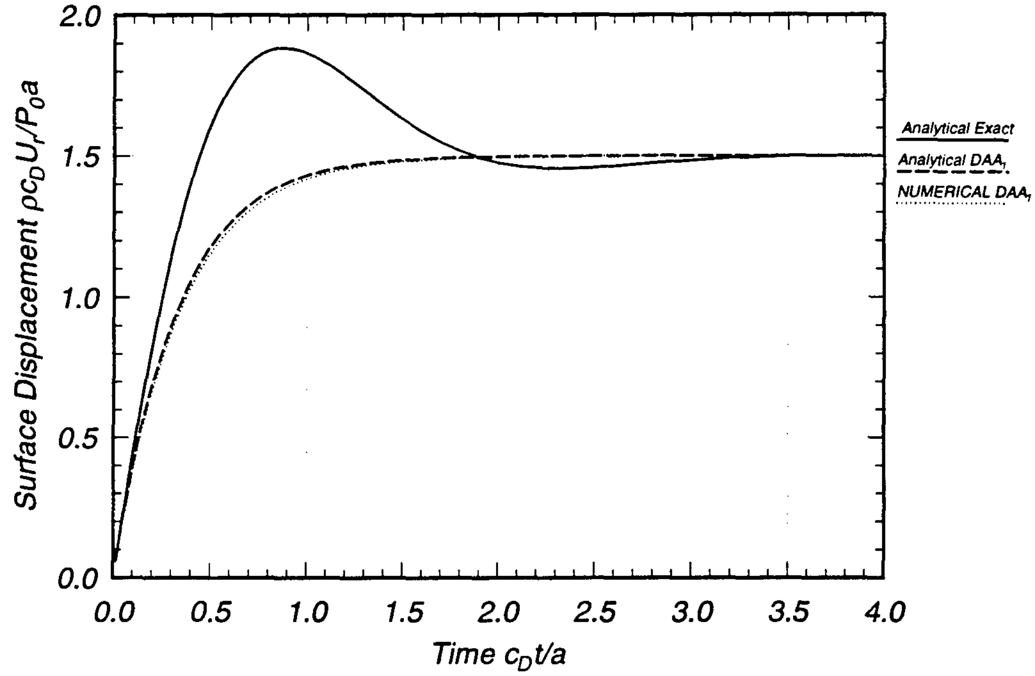

Figure 8-2. Exact and DAA$_1$ results for spherical cavity in an elastic medium subjected to an internal step pressure.

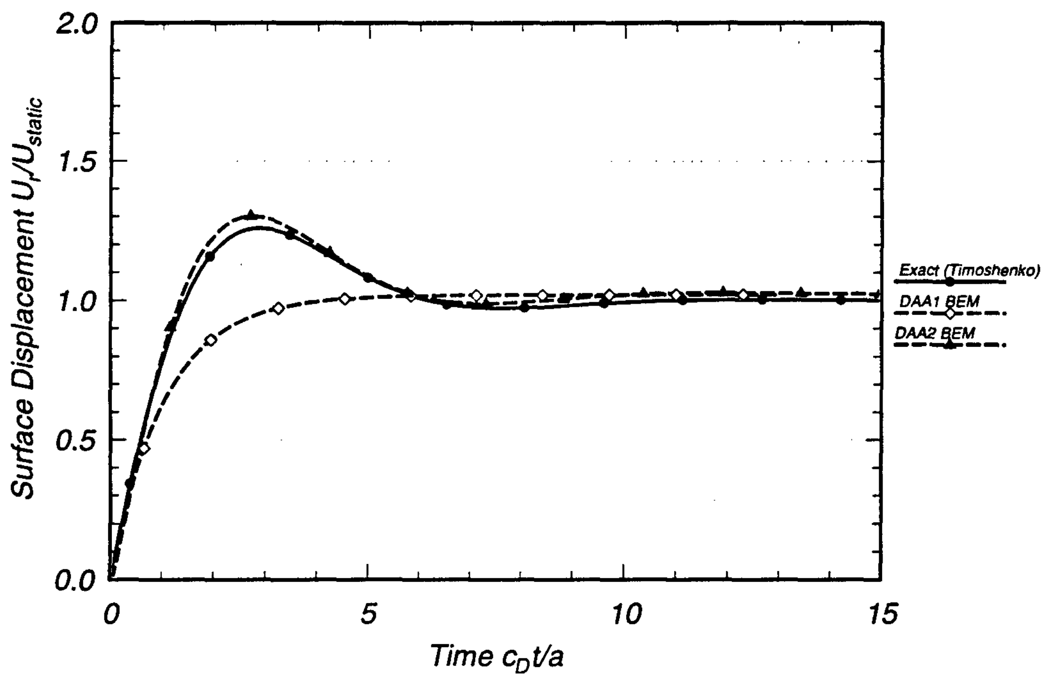

Figure 8-3. Exact, DAA$_1$, and DAA$_2$ radial displacement of a spherical cavity in an infinite elastic medium subjected to an internal step pressure.

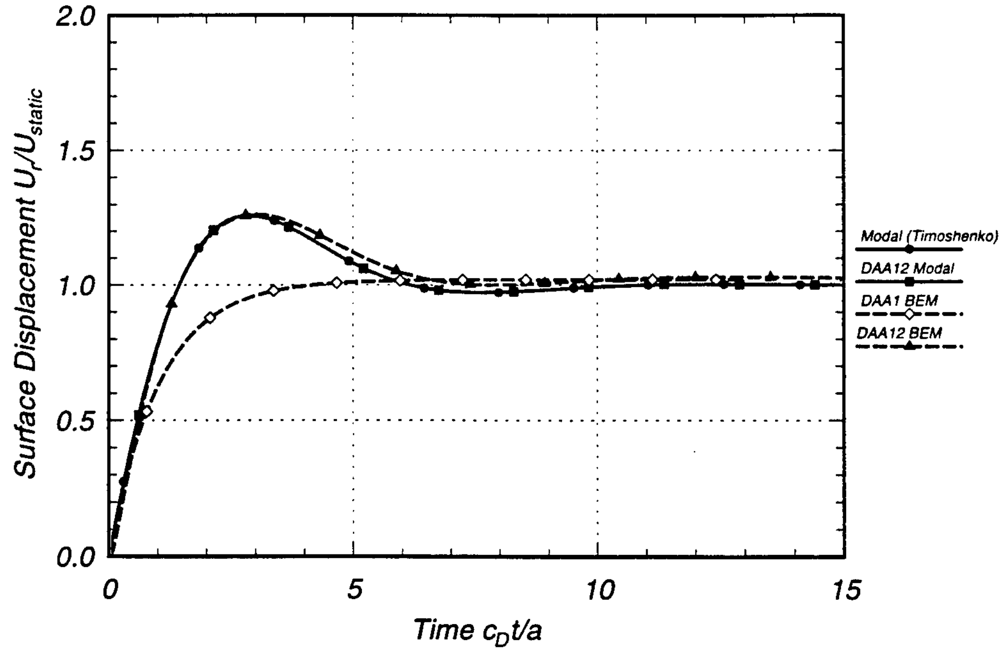

Figure 8-4. Exact, DAA_1, and DAA_{1-2} radial displacement of a spherical cavity in an infinite elastic medium subjected to an internal step pressure.

terms of $O(s^3)$, whereas the DAA_2 and DAA_{1-2} relations, (7.52) and (7.48), include terms only through $O(s^2)$.

The modal solution for this case is determined by using τ_1 equal to p_0 in equation (7.36) and σ_1 equal to $2p_0$. No σ_1 to τ_1 ratio other than two will produce a stable late-time result. Figure 8-5 presents a comparison of radial displacement responses for the exact relation (7.36), the DAA_2 relation (7.52), and the DAA_1 relation (7.46). Figure 8-6 compares the meridional (tangential) displacement solutions for these relations. Agreement between the exact and DAA_2 modal results is excellent.

Finally, Figures 8-7 and 8-8 compare results from the mixed-order DAA, DAA_{1-2}, (modal and BEM), with exact and DAA_1. We see that the essentially coincident modal and BEM DAA_{1-2} histories deviate modestly from the exact history.

8.4 SPHERICAL CAVITY/ HALF–SPACE/ STEP PRESSURE PROBLEM.

The third problem is a *spherical cavity embedded in a semi–infinite elastic medium and excited by an internal step pressure.* This problem is very difficult for doubly asymptotic approximations, at least as formulated to date. Only the late-time approximations have terms that include the effect of the free surface. Specifically, the dynamic free-surface effect is manifested only in the half–space terms of $\tilde{\mathbf{A}}$, $\tilde{\mathbf{B}}$, and $\tilde{\Gamma}$ [see (5.7), (5.8), (5.12), and (5.14)]. The reflection of the waves from the free surface occurs at intermediate times if the cavity is fairly close, but not immediately adjacent, to the surface.

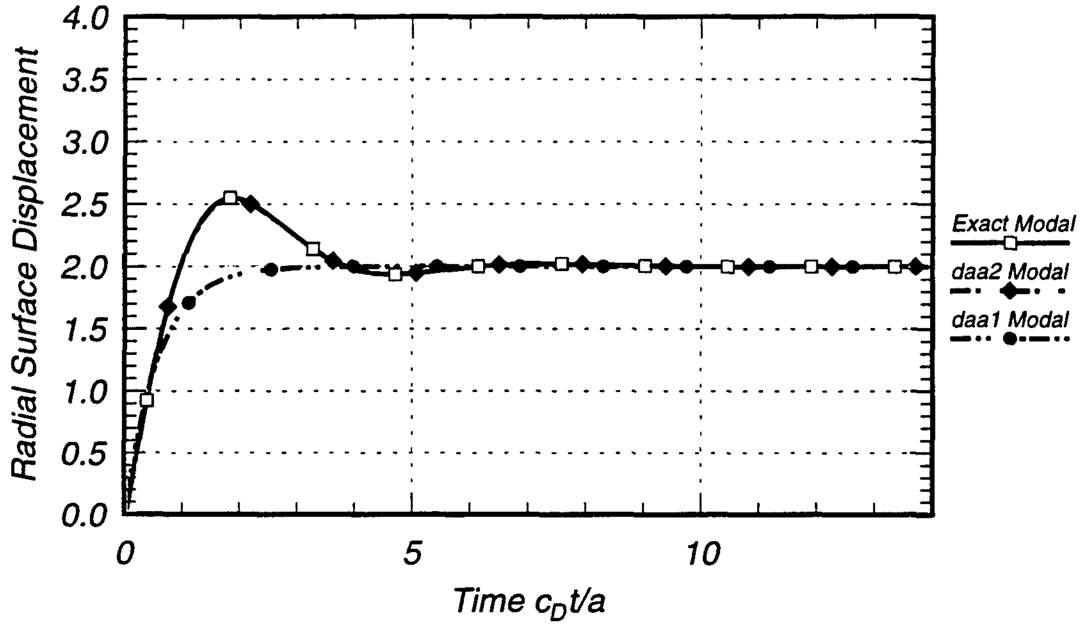

Figure 8-5. Exact, DAA$_1$, and DAA$_2$ radial displacements of a spherical cavity in an infinite elastic medium subjected to n=1 step tractions.

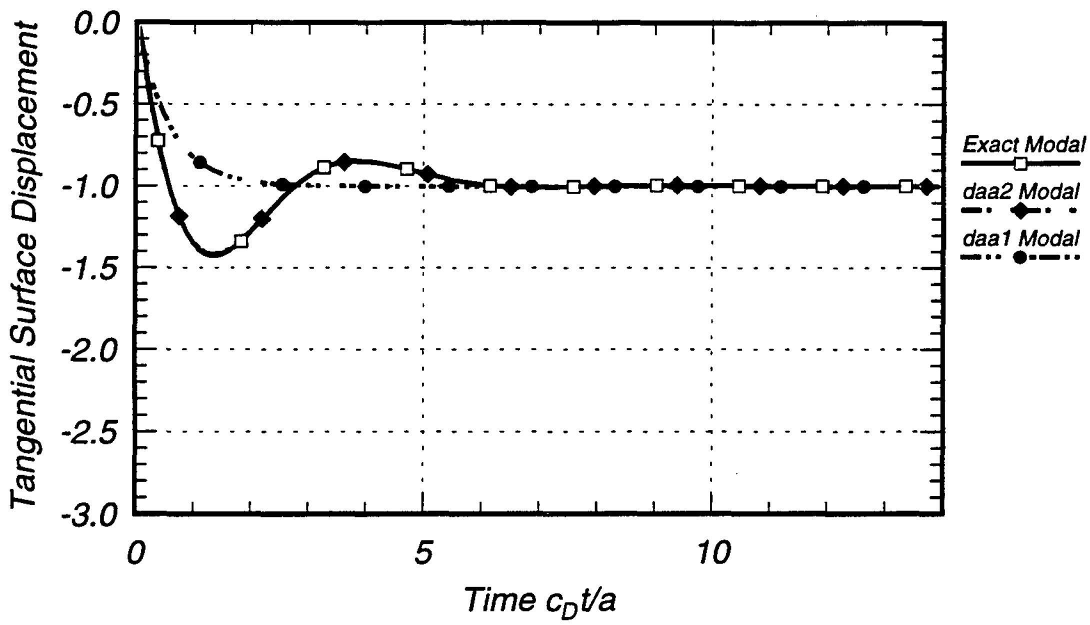

Figure 8-6. Exact, DAA$_1$, and, DAA$_2$ tangential displacements of a spherical cavity in an infinite elastic medium subjected to $n = 1$ step tractions.

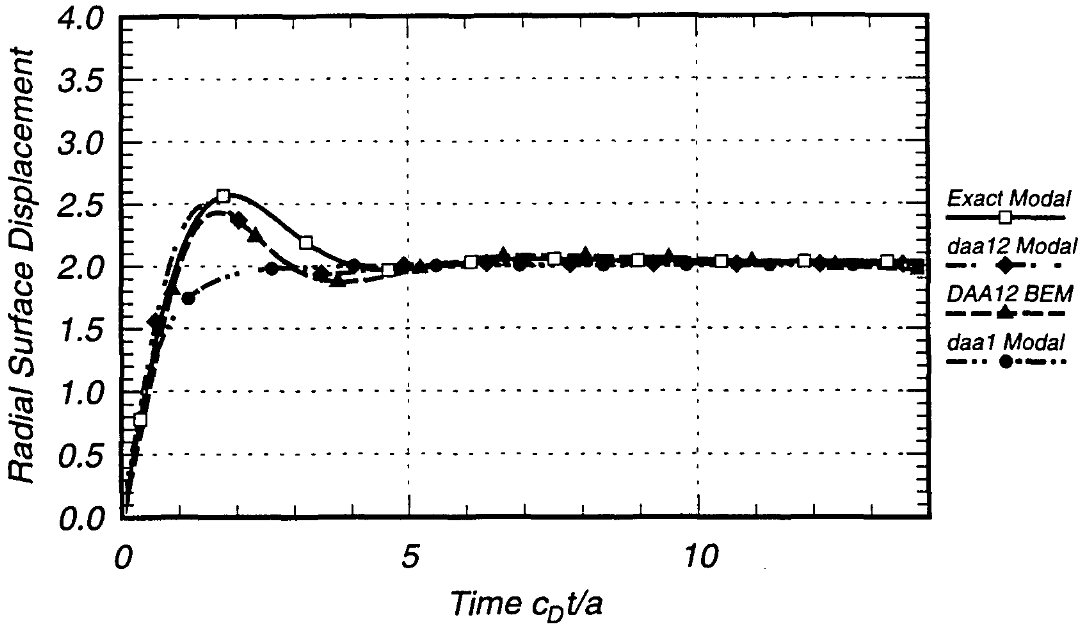

Figure 8-7. Exact, DAA_1, and DAA_{1-2} radial displacement of a spherical cavity in an infinite elastic medium subjected to $n = 1$ step internal tractions.

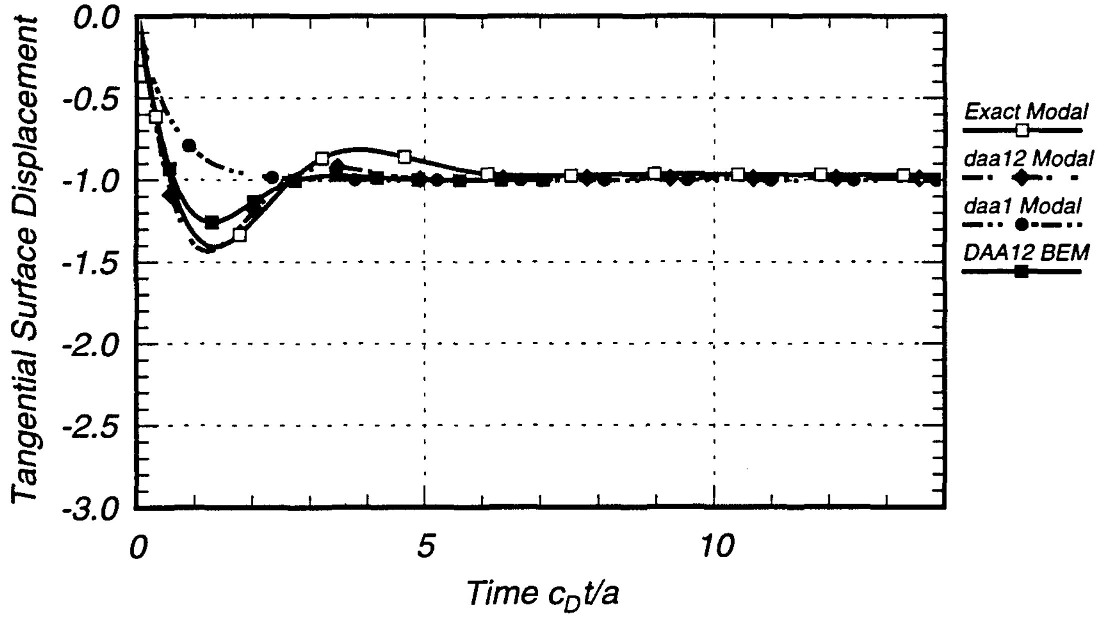

Figure 8-8. Exact, DAA_1, and DAA_{1-2} tangential displacements of a spherical cavity in an elastic medium subjected to a $n = 1$ step internal tractions.

This problem does not possess radial symmetry, and does not posses an analytical solution. However, a boundary–element solution based on numerical inversion of Laplace transforms has been generated by Manolis and Ahmad (Manolis and Ahmad., 1988), and an analytical solution to the related static problem exists (Bonefed, 1990). In terms of the geometry shown in Figure 8-9, the latter solution is

$$\begin{aligned} u_r &= P_0 a^3 \left\{ (1-2\nu)\frac{r}{R^{*3}} - \frac{3z(z+d)r}{R^{*5}} \right. \\ &\qquad \left. + \frac{1}{2}\left[\frac{r}{R'^3} + \frac{r}{R^{*3}}\right] \right\} \\ u_z &= P_0 a^3 \left\{ 2(1-2\nu)\frac{(z+d)}{R^{*3}} - \frac{z}{R^{*3}} + \frac{3z(z+d)^2}{R^{*5}} \right. \\ &\qquad \left. + \frac{1}{2}\left[\frac{(z+d)}{R'^3} + \frac{(z+d)}{R^{*3}}\right] \right\} \end{aligned} \tag{8.7}$$

where

$$\begin{aligned} R' &= \sqrt{r^2 + (z - z_0)^2} \\ R^* &= \sqrt{r^2 + (z + z_0)^2}. \end{aligned}$$

Numerical DAA_1 and numerical inversion solutions for this problem are shown in Figures 8-10–8-12, along with the late–time static asymptotes given by (8.7); the physical parameters specified are the same as those previously given for the infinite–domain problem. Figure 8-10 pertains to the top of the cavity, *i.e.*, the point on the cavity surface closest to the free surface of the elastic half–space. The numerical inversion solution by Manolis and Ahmad shows the pressure wave reflected from the free surface, at $^{c_D t}\!/_a = 2$. The effects of the reflected shear and Rayleigh wave at $^{c_D t}\!/_a = 2.73$ and $^{c_D t}\!/_a = 3.4$, respectively, complicate the response. Figure 8-11 pertains to a point 90° around, and Figure 8-12 pertains to the bottom of the cavity. These figures show that the DAA_1 solutions agree with the numerical inversion solutions at early time and appear to approach the correct late–time asymptotes. Unfortunately, the numerical inversion solutions do not extend far enough in time to allow a completely satisfactory comparison.

We also generated results from halfspace-DAA_2 for the spherical cavity in a semi-infinite elastic domain subjected to an internal step pressure. We show the DAA_2 radial displacements at three locations on the spherical surface, $\theta = 0°$, $\theta = 90°$, and $\theta = 180°$ in Figures 8-13- 8-15. We compare these solutions with the corresponding numerical inversion solutions (Manolis and Ahmad., 1988) and the static asymptotes ($t = \infty$). All radial displacements have been divided by the exact static solution for a spherical cavity in an infinite elastic domain, $u_{static} = \frac{Pa}{4\mu}$.

Radial displacement response at $\theta = 0°$ (closest to free surface) shows the effect of the dilatational wave reflecting from the free surface at $\frac{c_D t}{a} = 2.0$. DAA_2 radial displacement response at $\theta = 90°$

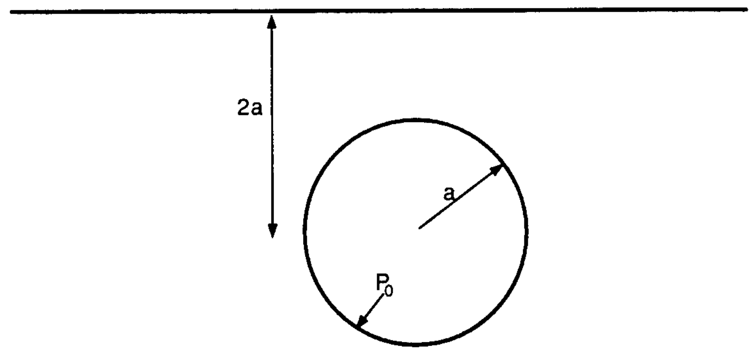

Figure 8-9. Geometry for a cavity embedded in a semi–infinite elastic medium.

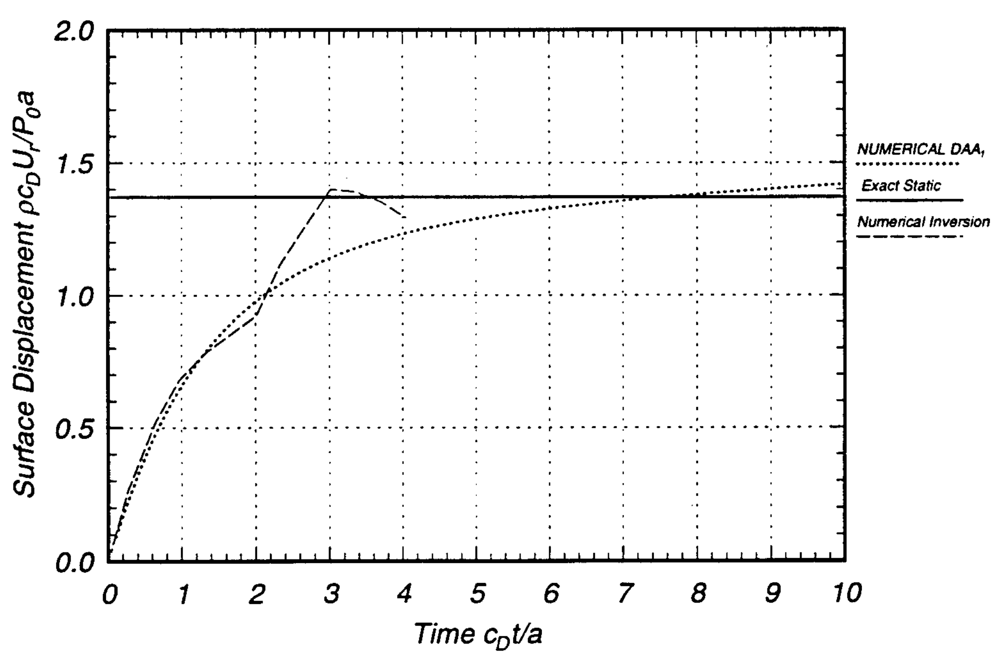

Figure 8-10. Radial displacement response of a step-pressurized cavity in a semi–infinite elastic medium ($\theta = 0°$, $d = a$).

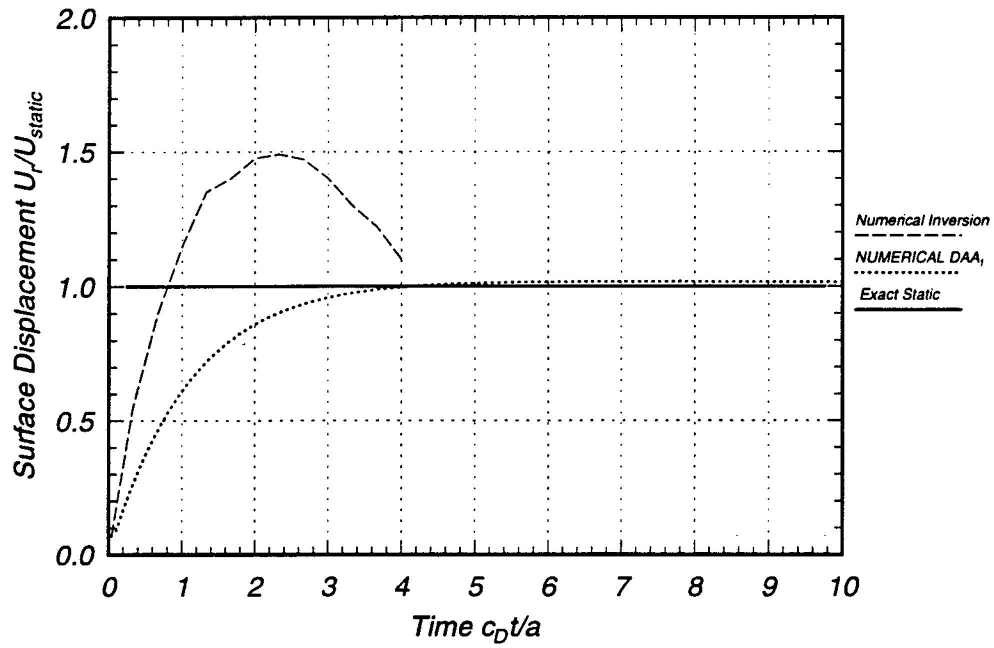

Figure 8-11. Radial displacement response of a step-pressurized cavity in a semi–infinite elastic medium ($\theta = 90°$, $d = 2a$).

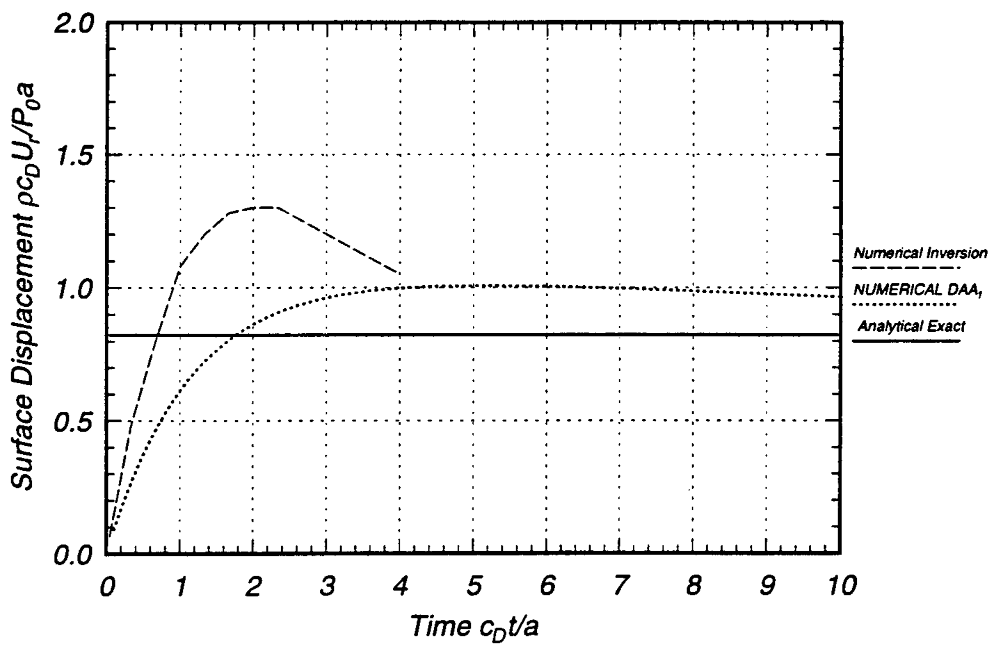

Figure 8-12. Radial displacement response of a step-pressurized cavity in a semi–infinite elastic medium ($\theta = 180°$, $d = 3a$).

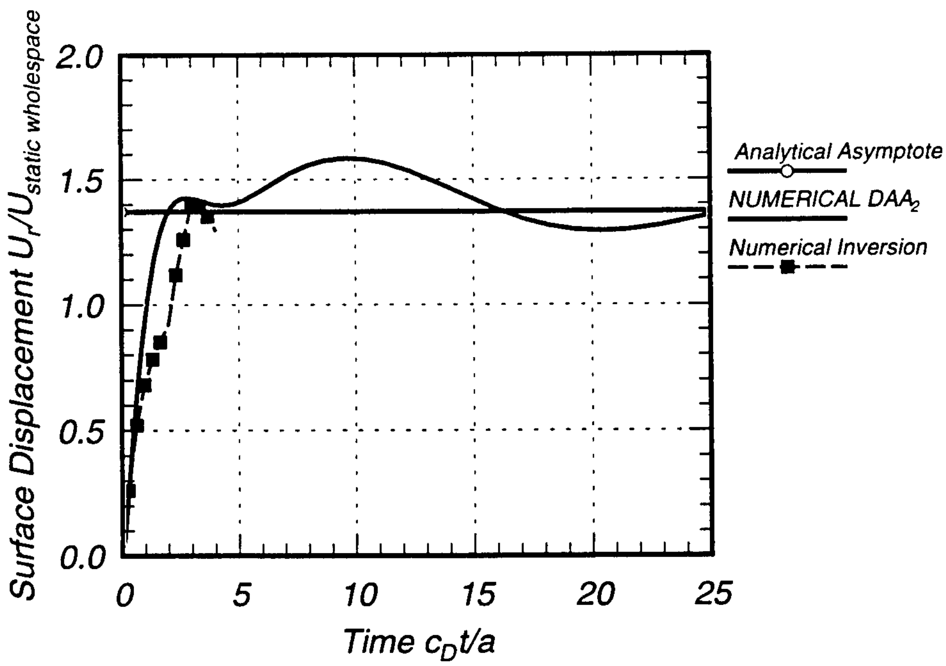

Figure 8-13. Radial displacement response of a step-pressurized cavity in a semi–infinite elastic medium with $DAA_2(\theta = 0°, d = a)$.

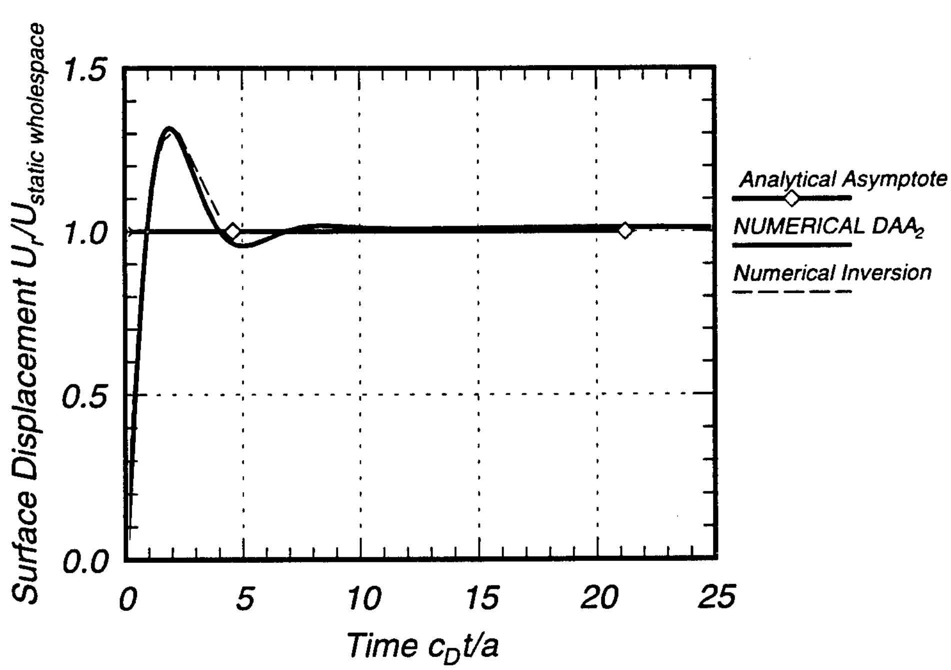

Figure 8-14. Radial displacement response of a step-pressurized cavity in a semi–infinite elastic medium with DAA_2 $(\theta = 90°, d = 2a)$.

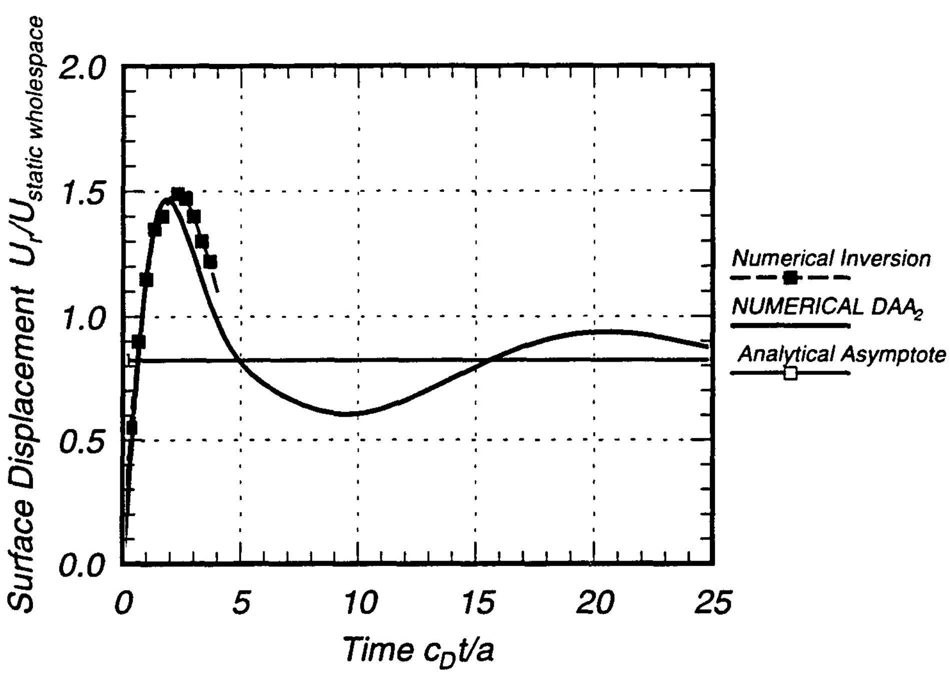

Figure 8-15. Radial displacement response of a step-pressurized cavity in a semi-infinite elastic medium with DAA$_2$ ($\theta = 180°$, $d = 3a$).

agrees well with the exact solution for a whole–space, see Section 8.2. Radial displacement response at $\theta = 180°$ exibits the greatest overshoot beyond the corresponding late-time asymptote.

8.5 STEP PRESSURE ON A HALF–SPACE WITH WHOLE–SPACE MATRICES.

The fourth (two-dimensional) canonical problem is a step pressure applied to a portion of the surface of an elastic half–space (Figure 8-16). Because of the spatial discontinuity of the load, a relief wave travels from each discontinuity toward $r = 0$. The problem has been studied analytically by Eason (Eason, 1966). The surface is flat so there is no curvature, $a = 1.61$, and the material properties are the same as those used previously. The surface is discretized using 36 elements. We terminated the model mesh at two different radii, $\frac{ar}{c_D} = 1.0$ (Manolis and Beskos, 1988) and $\frac{ar}{c_D} = 16.0$. We compare results for the normal displacement at $r = 0$ for the two boundary radii in Figure 8-17. Eason's analytical result is suspect at $\frac{c_D t}{a} = 1.8$; the discontinuous displacement is probably caused by the inversion method used (Kim and Soedel, 1988). Note that the result from the second-order whole–space DAA does have a smooth response. The smaller radius mesh begins to diverge significantly at $\frac{c_D t}{a} = 5.0$. The second-order DAA response is linear until $\frac{c_D t}{a} = 1.0$, when a dilatational wave reaches the center ($r = 0$) from the edge of the loaded area. When $\frac{c_D t}{a} > 1.0$ the second-order DAA strongly resembles a first-order DAA, *i.e. it produces no elastic overshoot.* This is because the surface is flat so the curvature terms in the second-order early-time approximations are zero for this problem. As expected the late-time (static) result is accurately found.

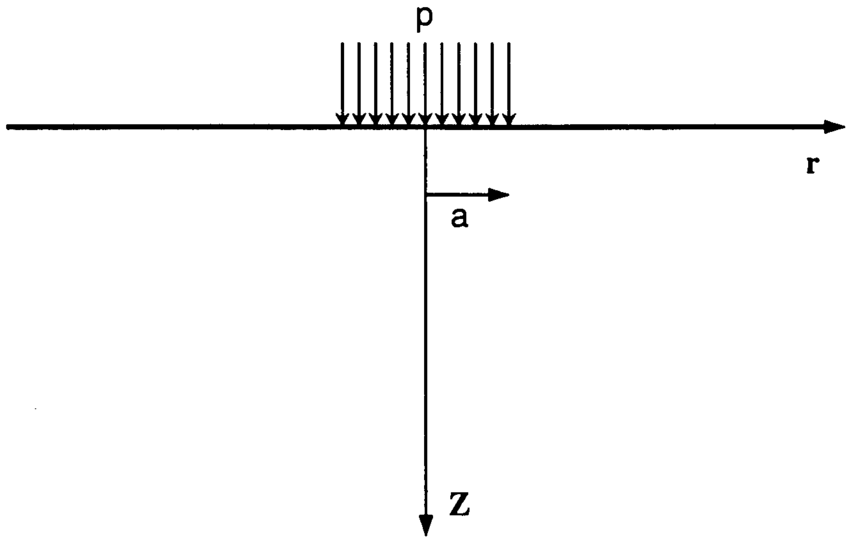

Figure 8-16. Normal step-load applied to an elastic half-space.

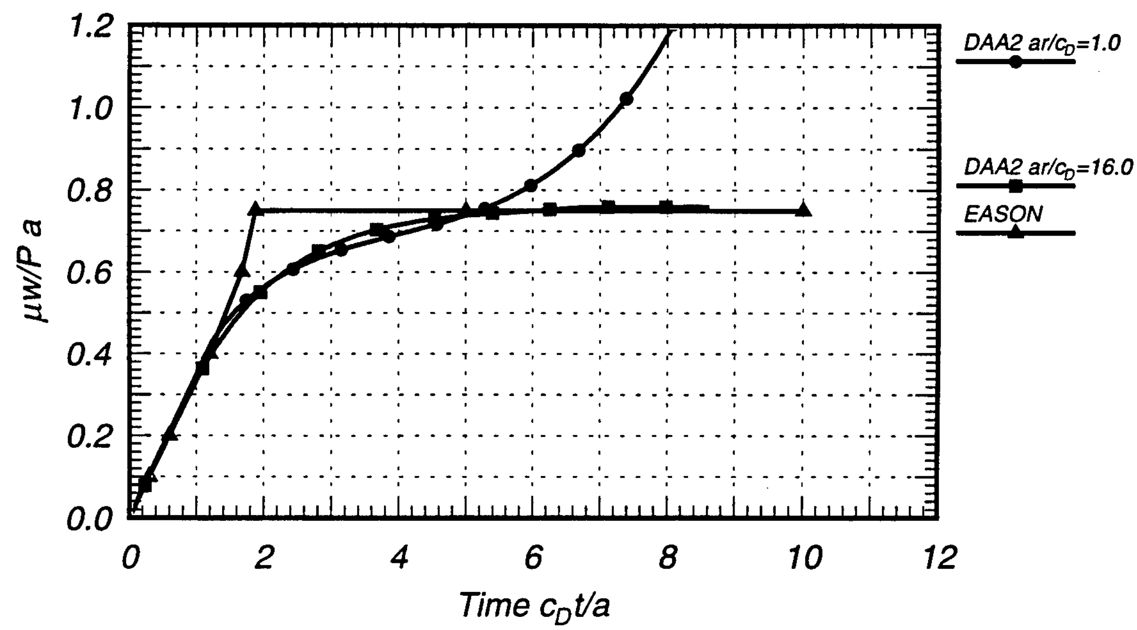

Figure 8-17. Normal displacement at $r = 0$ for normal step load applied to an elastic half–space with whole–space DAA_2.

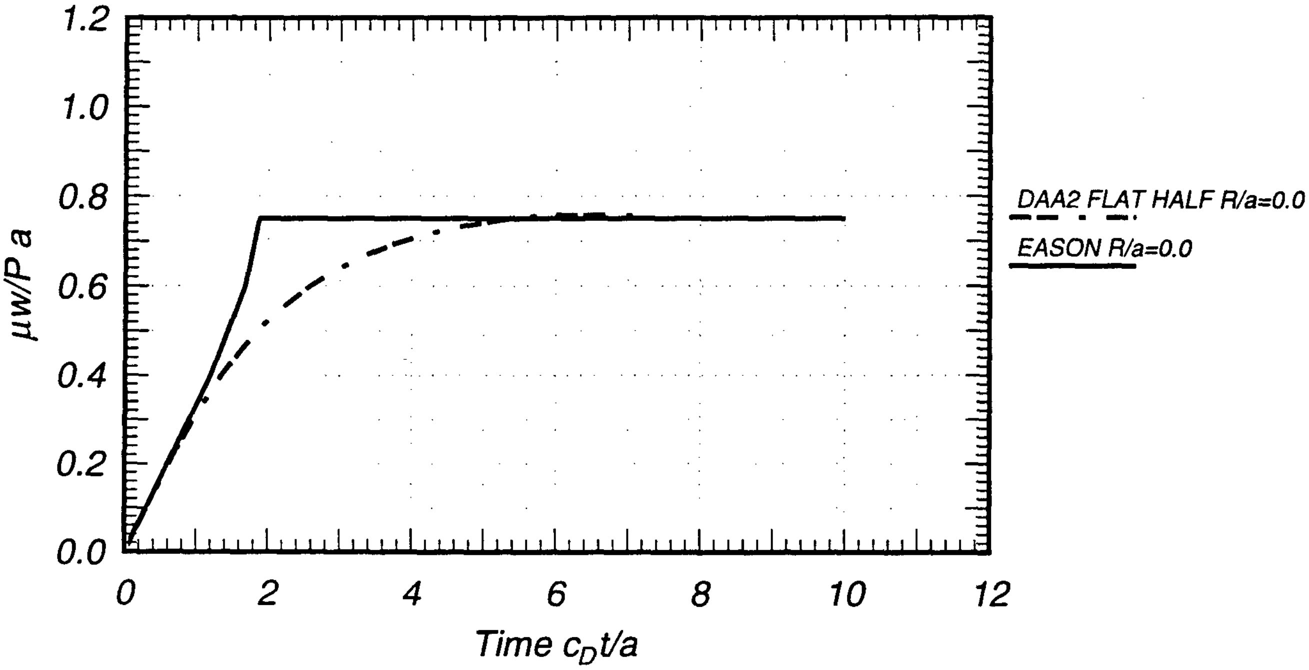

Figure 8-18. Normal displacement at $r = 0$ for normal step-load applied to an elastic half–space with half–space DAA_2.

8.6 STEP PRESSURE ON A HALF–SPACE WITH HALF–SPACE MATRICES.

The last comparison also pertains to the half–space problem. The discretatization for this problem consisted of 36 elements. Figure 8-18 shows normal-displacement response at $r = 0$ from the half–space DAA_2 along with Eason's analytical result. The half–space DAA_2 response is almost identical to the whole–space DAA_2 response discussed previously, but was computed in about one-fourth the time because no boundary elements were needed for the unloaded surface area.

SECTION 9

CONCLUSION

This report documents a systematic formulation and an analytical and numerical evaluation of first-order and second-order doubly asymptotic approximations for computational boundaries in the solution of transient soil-structure interaction problems. Specifically,

1. The early-time (high-frequency) approximations for an acoustic medium, systematically formulated by Felippa (Felippa, 1980b), were extended to isotropic elastic domains.

2. Ray elastodynamics, developed by H. B. Keller and J. B. Keller (Keller, 1958), (Keller, 1964), (Ahluwalia *et al.*, 1969), was also employed in the formulation of the early-time approximations.

3. The first- and second-order late-time (low-frequency) approximations for infinite and semi-infinite elastic media were systematically formulated from the elastodynamic boundary-integral equations of Cruse and Rizzo (Cruse and Rizzo, 1968) and the half-space operators of Banerjee and Mamoon (Banerjee and Mamoon, 1990).

4. The first-order DAA's for both infinite and semi-infinite isotropic elastic media were systematically formulated; the operator matching method of Nicholas-Vullierme (Nicholas-Vullierme, 1991) and of Geers and Zhang (Geers and Zhang, 1991) was used to derive these DAA's, which support the heuristic formulation of Underwood and Geers (Underwood and Geers, 1981).

5. The second-order DAA's for both infinite and semi-infinite isotropic elastic media were systematically formulated using the operator-matching method.

6. Mixed-order DAA's were formulated for both inifinite and semi-infinite isotropic elastic media; each combines a first-order low-frequency approximation with a second-order high-frequency approximation.

7. Finite-element discretization was introduced to configure the DAA formulas for boundary-element solution; pertinent computer programs were written to generate numerical results.

8. Exact, DAA_1, DAA_2 and DAA_{1-2} modal computational boundary relations were derived for dilatational, rotational and translational motions of a spherical boundary in an infinite isotropic elastic medium.

9. Boundary-element DAA_1 and DAA_{1-2} results for suddenly pressurized spherical cavities embedded in infinite and semi-infinite elastic media were generated; the DAA results were compared with corresponding analytical results from Timoshenko and Goodier (Timoshenko and Goodier, 1970), Manolis and Ahmad (Manolis and Ahmad., 1988), Bonefed (Bonefed, 1990), and with analytical results generated herin.

10. Boundary-element DAA_2 results for a pressure load applied suddenly to a portion of the surface of an elastic semi-infinite domain were generated; these were compared with results reported by Eason (Eason, 1966).

The principal conclusions reached in this study are:

1. First-order doubly asymptotic approximations are useful as computational boundaries for elastic media, but they cannot predict the response overshoot that characterizes many problems.

2. Second-order doubly asymptotic approximations are quite useful as computational boundaries for elastic media, successfully predicting response overshoot.

3. Half–space DAA's are much more efficient than whole-space DAA's for half-space problems because the former do not require discretization of unloaded free-surface areas.

4. The whole-space DAA_2 is exact for dilatational and rotational motion of a spherical surface; for the translational cases studied, the modal DAA_2 results agree perfectly with the corresponding exact results.

5. The mixed-order whole-space DAA (DAA_{1-2}) is exact for dilatational and rotational motion of a spherical surface; it is less accurate than the whole-space DAA_2 for translational motion.

SECTION 10

REFERENCES

J. D. Achenbach et al. *Ray Methods For Waves in Elastic Solids.* Pittman Publishing, Inc, Marshfield, MA, USA, 1982. (UNCLASSIFIED)

J. D. Achenbach. *Wave Propagation in Elastic Solids.* North Holland, New York, 1973. (UNCLASSIFIED)

D. S. Ahluwalia, J. B. Keller, and E. Resende. Reflection of elastic waves from cylindrical surfaces. *Jour Math Mech*, 19:93–105, 1969. (UNCLASSIFIED)

G. Arfken. *Mathematical Methods for Physics.* Academic Press, New York, 1970. (UNCLASSIFIED)

P. K. Banerjee and S. M. Mamoon. A fundemental solution due to a periodic point force in the interior of an elastic half-space. *Earthquake Engineering and Structural Dynamics*, 19:91–105, 1990. (UNCLASSIFIED)

M. Bonefed. Axisymmetric deformation of a thermo-poro-elastic halfspace; inflation of a magma chamber. *Geophys J. Inter*, 22:289–299, 1990. (UNCLASSIFIED)

C. A. Brebbia et al. *Boundary Element Techniques: Theory and Application in Engineering.* Springer-Verlag, Berlin, 1984. (UNCLASSIFIED)

R. D. Cook, D. S. Malkus, and M. E. Plesha. *Concepts and Applications of Finite Element Analysis.* John Wiley And Sons, New York, 1989. (UNCLASSIFIED)

T. A. Cruse and F. J. Rizzo. A direct formulation and numerical solution of the general transient elastodynamic problem. *Journal of Mathematical Analysis & Applications*, 22:244–259, 1968. (UNCLASSIFIED)

J. M. Doyle. Integration of the Laplace transformed equations of classical elastokinetics. *Journal of Mathematical Analysis and Applications*, 13:118–131, 1966. (UNCLASSIFIED)

G. Eason. The displacements produced in an elastic half-space by a suddenly applied surface force. *Journal of the Institute for Mathematical Analysis & Applications*, 2:299–326, 1966. (UNCLASSIFIED)

A. Cemal Eringen and Erdogan S. Suhubi. *Elastodynamics – Linear Theory Vol 2.* Acadamic Press, New York, 1975. (UNCLASSIFIED)

C. A. Felippa. *Top-Down Derivation of Doubly-Asymptotic Approximation for Structure-Fluid Interaction Analysis in Innovative Numerical Analysis for Engineering Sciences.* University Press of Virginia, Charllottesville, 1980. (UNCLASSIFIED)

C.A. Felippa. A family of early time approximations for fluid structure interaction. *Journal Applied Mechanics*, 47:703–708, 1980. (UNCLASSIFIED)

F. G. Freidlander. *Sound Pulses*. Cambridge University Press, London, 1958. (UNCLASSIFIED)

T. L. Geers and C. A. Felippa. Doubly asymptotic approximation for vibration analysis of submerged structures. *Journal of Acoustic Society of America*, 73:1152–1159, 1983. (UNCLASSIFIED)

T. L. Geers and P. Zhang. Doubly asymptotic approximations for electromagnetic scattering problems. In *Boundary Element Methods in Applied Mechanics*, pages 357–369. Peramon Press, 1988. (UNCLASSIFIED)

T. L. Geers and P. Zhang. Doubly asymptotic approximations for internal and external acoustic domains: Formulation. *Dynamic Response of Structures to High-Energy Excitations*, AMD-127, ASME, New York:13–26, 1991. (UNCLASSIFIED)

T L. Geers. Residual potential and approximate methods for three-dimensional fluid-structure interaction problems. *Journal of Acoustical Society of America*, 49:1505–1510, 1971. (UNCLASSIFIED)

T. L. Geers. Doubly asymptotic approximations for transient motions of submerged structures. *Journal of Acoustic Society of America*, 64:1500–1508, 1978. (UNCLASSIFIED)

D. Givoli and J. B. Keller. Non-reflecting boundary conditions for elastic waves. *Wave Motion*, 12:261–279, 1990. (UNCLASSIFIED)

D. Givoli. A spatially exact non-reflecting boundary condition for time dependent problems. *Computer Methods in Applied Mechanics and Engineering*, 95:97–113, 1992. (UNCLASSIFIED)

T J. R. Hughes. *The Finite Element Method*. Prentice-Hall, Englewood Cliffs New Jersey, 1987. (UNCLASSIFIED)

L. F. Kallivokas, B. Bielak, and R. C. MacCamy. Symmetric local absorbing boundaries in time and space. *Journal of Engineering Mechanics*, 117:2027–2048, 1991. (UNCLASSIFIED)

J. B. Keller. A geometrical theory of diffraction. *Calculus of Variations and Its Applications*, Proc of Eigth Symp in Appl Math:27–52, 1958. (UNCLASSIFIED)

H. B. Keller. Propagation of stress discontinuities in inhomogeneous elastic media. *SAIM Review*, 6:356–382, 1964. (UNCLASSIFIED)

J. S. Kim and W. Soedel. On the response of three–dimensional elastic bodies to distributed dynamic pressures, part i: Half space. *Journal of Sound And Vibration*, 126(2):279–295, 1988. (UNCLASSIFIED)

G. Kirchhoff. *Annuals Phys. Chem.*, 18, 1883. (UNCLASSIFIED)

A. E. H. Love. The propagation of wave motion in an isotropic elastic solid medium. *Proceedings of London Mathamatical Society*, 2:213–344, 1904. (UNCLASSIFIED)

A. E. H. Love. Wave-motions with discontinuities of wave-fronts. *Proceedings of London Mathamatical Society*, 2, 1904. (UNCLASSIFIED)

A. E. H. Love. *A Treatise on the Mathematical Theory of Elasticity.* Dover, New York, 1944. (UNCLASSIFIED)

G. D. Manolis and S. Ahmad. Ground motions resulting from a pressurized cavity. *Wave Motion*, 10:465–478, 1988. (UNCLASSIFIED)

G. D. Manolis and D. E. Beskos. *Boundary Element Methods in Elastodynamics.* Unwin Hyman Ltd, London, 1988. (UNCLASSIFIED)

G. D. Manolis. A comparative study of the boundary element method approaches to problems in elastodynamics. *International Journal of Numerical Methods in Engineering*, 19:73–91, 1983. (UNCLASSIFIED)

I. C. Mathews and T. L. Geers. A doubly asymptotic, nonreflecting boundary for ground shock analysis. *J. Applied Mech*, 54:489–497, 1987. (UNCLASSIFIED)

I. C. Mathews. Private communication. Sept 1990. (UNCLASSIFIED)

R. D. Mindlin. Force at a point in the interior of an semi–infinite solid. *Jounal of Applied Physics*, 7:195–202, 1936. (UNCLASSIFIED)

P. Moon and D. E. Spencer. *Field Theory Handbook.* Springer-Verlag, Berlin, 1961. (UNCLASSIFIED)

B. Nicholas-Vullierme. A contribution to doubly asymptotic approximations: An operator top-down derivation. *Jounal of Vibration and Acoustics*, 113:409–415, 1991. (UNCLASSIFIED)

A. A. Oberai. *Transient Response Analysis of Cylindrical and Spherical Shells Embedded in an Elastic Medium: Residual Potential and Doubly Asymptotic Solutions.* University of Colorado, Boulder CO, February 1994. (UNCLASSIFIED)

S. D. Poisson. *Paris Mem Institute*, 3, 1820. (UNCLASSIFIED)

Y. H. Pow and C. C. Mow. *Diffraction of Elastic Waves and Dynamic-Stress Concentration.* Crane Russak, 1972. (UNCLASSIFIED)

E. Sternburg and R. A. Eubanks. On stress functions for elastokinetics and the integration of the repeated wave equation. *Quarterly Applied Math.*, 15, 1957. (UNCLASSIFIED)

G. G. Stokes. On the dynamical theory of diffraction. *Transactions of the Cambridge Philosophical Society*, 9:1–62, 1849. (UNCLASSIFIED)

Sir W. Thomson. Cambridge and dublin math. j. *reprinted in Math and Phys. Papers*, 1:97, 1948. (UNCLASSIFIED)

S. P. Timoshenko and J. N. Goodier. *Theory of Elasticity.* McGraw-Hill, New York, 1970. (UNCLASSIFIED)

H. Uberall et al. Application fo the singularity expansion method to elastic wave scattering. *Applied Mechanics Review*, 43(10):235–249, 1990. (UNCLASSIFIED)

P. G. Underwood and T. L. Geers. Doubly asymptotic boundary element analysis of dynamic soil-structure interaction. *Int. J. Solids Struc*, 17:687–697, 1981. (UNCLASSIFIED)

R G. Whirley. *DYNA3D, A Nonlinear Explicit Three-Dimensional Finite Element Code for Solid and Structural Mechanics.* Lawerence Livermore National Laboratory, Livermore CA, 1991. (UNCLASSIFIED)

C. F. Ying and R. Truell. Scattering of a plane longitudinal wave by a spherical obstacle in an isotropically elastic solid. *Journal of Applied Physics*, 27:1086–1097, 1956. (UNCLASSIFIED)

APPENDIX

TENSOR OPERATORS FOR HALF SPACE

The following are the first group of $\vec{U}$ operators that pertain to the cylindrical coordinate system.

$$
\begin{aligned}
U^1_{rz} &= K_1\left[-B_1\left(\frac{\partial R_1}{\partial r}\right)\left(\frac{\partial R_1}{\partial z}\right)\right] \\
U^1_{zz} &= K_1\left[A_1 - B_1\left(\frac{\partial R_1}{\partial z}\right)^2\right] \\
U^2_{rz} &= K_2\left[-B_2\left(\frac{\partial R_2}{\partial r}\right)\left(\frac{\partial R_2}{\partial z}\right)\right] \\
U^2_{zz} &= K_2\left[A_2 - B_2\left(\frac{\partial R_2}{\partial z}\right)^2\right] \\
U^3_{rz} &= K_3\left[A_3\left(\frac{\partial R_2}{\partial z}\right)^2 - B_3\right]\left(\frac{\partial R_2}{\partial r}\right) \\
U^3_{zz} &= K_3\left[A_3\left(\frac{\partial R_2}{\partial z}\right)^2 - C_3\right]\left(\frac{\partial R_2}{\partial z}\right) \\
U^4_{rz} &= K_4\left[B_4\left(\frac{\partial R_2}{\partial r}\right)\right] \\
U^4_{zz} &= K_4\left[B_4\left(\frac{\partial R_2}{\partial z}\right)\right] \\
U^5_{rz} &= K_5\int_{\xi=-c}^{-\infty}\left[B_5\left(\frac{\partial R_3}{\partial r}\right)\right]d\xi \\
U^5_{zz} &= K_5\int_{\xi=-c}^{-\infty}\left[B_5\left(\frac{\partial R_3}{\partial z}\right)\right]d\xi \\
U^6_{rz} &= K_6\left[A_6\left(\frac{\partial R_2}{\partial r}\right)\left(\frac{\partial R_2}{\partial z}\right)\right] \\
U^6_{zz} &= K_6\left[B_6 + A_6\left(\frac{\partial R_2}{\partial z}\right)\right],
\end{aligned}
\tag{A.1}
$$

where

$$K_1 = \frac{1}{4\pi\mu} \qquad K_2 = \frac{3-4\nu}{4\pi\mu} \qquad K_3 = -\frac{c}{2\pi\mu}$$
$$K_4 = \frac{c(1-2\nu)}{\pi\mu(3-4\nu)} \quad K_5 = \frac{(1-\nu)(1-2\nu)}{\pi\mu(3-4\nu)} \quad K_6 = -\frac{c^2}{2\pi\mu(3-4\nu)}$$
$$R = (r_i r_i)^{\frac{1}{2}} \qquad R_2 = (r_i' r_i')^{\frac{1}{2}} \qquad R_3 = \{r^2 + (z+\xi)^2\}^{\frac{1}{2}}$$

$$A_1 = -\frac{{c_S}^2 \left(\frac{{c_D}^2}{{R_1}^2 s^2} + \frac{c_D}{R_1 s}\right)}{{c_D}^2 e^{\frac{R_1 s}{c_D}} R_1} + \frac{1 + \frac{{c_S}^2}{{R_1}^2 s^2} + \frac{c_S}{R_1 s}}{e^{\frac{R_1 s}{c_S}} R_1}$$

$$B_1 = -\frac{{c_S}^2 \left(1 + \frac{3{c_D}^2}{{R_1}^2 s^2} + \frac{3c_D}{R_1 s}\right)}{{c_D}^2 e^{\frac{R_1 s}{c_D}} R_1} + \frac{1 + \frac{3{c_S}^2}{{R_1}^2 s^2} + \frac{3c_S}{R_1 s}}{e^{\frac{R_1 s}{c_S}} R_1}$$

$$A_2 = A_1$$

$$B_2 = B_1$$

$$A_3 = -\frac{{c_S}^2 \left(6 + \frac{15{c_D}^2}{{R_2}^2 s^2} + \frac{15c_D}{R_2 s} + \frac{R_2 s}{c_D}\right)}{{c_D}^2 e^{\frac{R_2 s}{c_D}} {R_2}^2} + \frac{6 + \frac{15{c_S}^2}{{R_2}^2 s^2} + \frac{15c_S}{R_2 s} + \frac{R_2 s}{c_S}}{e^{\frac{R_2 s}{c_S}} {R_2}^2}$$

$$B_3 = -\frac{{c_S}^2 \left(1 + \frac{3{c_D}^2}{{R_2}^2 s^2} + \frac{3c_D}{R_2 s}\right)}{{c_D}^2 e^{\frac{R_2 s}{c_D}} {R_2}^2} + \frac{1 + \frac{3{c_S}^2}{{R_2}^2 s^2} + \frac{3c_S}{R_2 s}}{e^{\frac{R_2 s}{c_S}} {R_2}^2}$$

$$C_3 = -\frac{{c_S}^2 \left(3 + \frac{9{c_D}^2}{{R_2}^2 s^2} + \frac{9c_D}{R_2 s}\right)}{{c_D}^2 e^{\frac{R_2 s}{c_D}} {R_2}^2} + \frac{4 + \frac{9{c_S}^2}{{R_2}^2 s^2} + \frac{9c_S}{R_2 s} + \frac{R_2 s}{c_S}}{e^{\frac{R_2 s}{c_S}} {R_2}^2}$$

$$B_4 = \frac{1 + \frac{3{c_S}^2}{{R_2}^2 s^2} + \frac{3c_S}{R_2 s}}{e^{\frac{R_2 s}{c_S}} {R_2}^2} - \frac{{c_S}^2 \left(2 + \frac{3{c_D}^2}{{R_2}^2 s^2} + \frac{3c_D}{R_2 s} + \frac{R_2 s}{c_D}\right)}{{c_D}^2 e^{\frac{R_2 s}{c_D}} {R_2}^2}$$

$$B_5 = B_4$$

$$A_6 = -\frac{6 + \frac{15{c_S}^2}{{R_2}^2 s^2} + \frac{15c_S}{R_2 s} + \frac{R_2 s}{c_S}}{e^{\frac{R_2 s}{c_S}} {R_2}^3} + \frac{{c_S}^2 \left(9 + \frac{15{c_D}^2}{{R_2}^2 s^2} + \frac{15c_D}{R_2 s} + \frac{4R_2 s}{c_D} + \frac{{R_2}^2 s^2}{{c_D}^2}\right)}{{c_D}^2 e^{\frac{R_2 s}{c_D}} {R_2}^3}$$

$$B_6 = \frac{1 + \frac{3{c_S}^2}{{R_2}^2 s^2} + \frac{3c_S}{R_2 s}}{e^{\frac{R_2 s}{c_S}} {R_2}^3} - \frac{{c_S}^2 \left(2 + \frac{3{c_D}^2}{{R_2}^2 s^2} + \frac{3c_D}{R_2 s} + \frac{R_2 s}{c_D}\right)}{{c_D}^2 e^{\frac{R_2 s}{c_D}} {R_2}^3}$$

The following are the second group of $\vec{U}$ operators that pertain to the Cartesian coordinate system.

$$
\begin{aligned}
U^1_{xx} &= L_1\left[P_1 - Q_1\left(\frac{\partial R_1}{\partial x}\right)^2\right] \\
U^1_{yz} &= L_1\left[-Q_1\left(\frac{\partial R_1}{\partial y}\right)\left(\frac{\partial R_1}{\partial x}\right)\right] \\
U^1_{xz} &= L_1\left[-Q_1\left(\frac{\partial R_1}{\partial x}\right)\left(\frac{\partial R_1}{\partial x}\right)\right] \\
U^2_{xx} &= L_2\left[P_2 - Q_2\left(\frac{\partial R_2}{\partial x}\right)^2\right] \\
U^2_{yz} &= L_2\left[-Q_2\left(\frac{\partial R_2}{\partial y}\right)\left(\frac{\partial R_2}{\partial x}\right)\right] \\
U^2_{xz} &= L_2\left[-Q_2\left(\frac{\partial R_2}{\partial x}\right)\left(\frac{\partial R_2}{\partial x}\right)\right] \\
U^3_{xx} &= L_3\left[P_3\left(\frac{\partial R_2}{\partial z}\right)^2 - S_3\right]\left(\frac{\partial R_2}{\partial x}\right) \\
U^3_{yx} &= L_3\left[P_3\left(\frac{\partial R_2}{\partial x}\right)^2 - Q_3\right]\left(\frac{\partial R_2}{\partial z}\right) \\
U^3_{zx} &= L_3\left[Q_3\left(\frac{\partial R_2}{\partial x}\right)\left(\frac{\partial R_2}{\partial y}\right)\left(\frac{\partial R_2}{\partial z}\right)\right] \\
U^4_{xx} &= L_4\int_{\xi=-c}^{-\infty}\left[P_4\left(\frac{\partial R_3}{\partial x}\right)^2 - Q_4\right]\left(\frac{\partial R_3}{\partial z}\right)d\xi \\
U^4_{yx} &= L_4\int_{\xi=-c}^{-\infty}\left[P_4\left(\frac{\partial R_3}{\partial x}\right)\left(\frac{\partial R_3}{\partial y}\right)\left(\frac{\partial R_3}{\partial z}\right)\right]d\xi
\end{aligned}
\qquad (A.2)
$$

$$
\begin{aligned}
U^4_{zx} &= L_4 \int_{\xi=-c}^{-\infty} \left[P_4 \left(\frac{\partial R_3}{\partial z} \right)^2 - S_4 \right] \left(\frac{\partial R_3}{\partial x} \right) d\xi \\
U^5_{xx} &= L_5 \left[P_5 + Q_5 \left(\frac{\partial R_2}{\partial x} \right)^2 \right] \\
U^5_{yx} &= L_5 \left[Q_5 \left(\frac{\partial R_2}{\partial x} \right) \left(\frac{\partial R_2}{\partial y} \right) \right] \\
U^5_{zx} &= L_5 \left[Q_5 \left(\frac{\partial R_2}{\partial x} \right) \left(\frac{\partial R_2}{\partial z} \right) \right] \\
U^6_{xx} &= L_6 \int_{\xi=-c}^{-\infty} \left[P_6 + Q_6 \left(\frac{\partial R_3}{\partial x} \right)^2 \right] (\xi - c) d\xi \\
U^6_{yx} &= L_6 \int_{\xi=-c}^{-\infty} \left[Q_6 \left(\frac{\partial R_3}{\partial x} \right) \left(\frac{\partial R_3}{\partial y} \right) \right] (\xi - c) d\xi \\
U^6_{zx} &= L_6 \int_{\xi=-c}^{-\infty} \left[Q_6 \left(\frac{\partial R_3}{\partial x} \right) \left(\frac{\partial R_3}{\partial z} \right) \right] (\xi - c) d\xi,
\end{aligned}
$$

where

$$
\begin{aligned}
L_1 &= K_1 \\
L_2 &= \frac{1}{4\pi\mu} \\
L_3 &= \frac{c}{2\pi\mu} \\
L_4 &= -\frac{(1-2\nu)}{2\pi\mu} \\
L_5 &= K_6 \\
L_6 &= -\frac{(1-\nu)(1-2\nu)}{\pi\mu(3-4\nu)}
\end{aligned}
$$

$$
\begin{aligned}
P_1 &= A_1 \\
Q_1 &= B_1 \\
P_2 &= A_2 \\
Q_2 &= B_2 \\
P_3 &= A_3 \\
Q_3 &= B_3 \\
S_3 &= -\frac{{c_S}^2\left(1+\frac{3\,{c_D}^2}{{R_2}^2\,s^2}+\frac{3\,c_D}{R_2\,s}\right)}{{c_D}^2\,e^{\frac{R_2\,s}{c_D}}\,{R_2}^2}+\frac{2+\frac{3\,{c_S}^2}{{R_2}^2\,s^2}+\frac{3\,c_S}{R_2\,s}+\frac{R_2\,s}{c_S}}{e^{\frac{R_2\,s}{c_S}}\,{R_2}^2} \\
P_4 &= P_3 \\
Q_4 &= Q_3 \\
S_4 &= S_3 \\
P_5 &= B_6 \\
Q_5 &= A_6 \\
P_6 &= P_5 \\
Q_6 &= Q_5
\end{aligned}
$$

DISTRIBUTION LIST

DSWA TR-96-46

DEPARTMENT OF DEFENSE

DEFENSE SPECIAL WEAPONS AGENCY
ATTN: PMPA, DR C GALLOWAY
2 CY ATTN: TRC
ATTN: WEL
ATTN: WEL, LTC A KUEHN
ATTN: WEL, MAJ DAVE MYERS
ATTN: WEL, MAJ T SMITH
ATTN: WEL, L WITTWER
ATTN: WEL, W ZIMMERS
2 CY ATTN: WELE, LTC JIM HODGE

DEFENSE TECHNICAL INFORMATION CENTER
2 CY ATTN: DTIC/OCP

FC DEFENSE SPECIAL WEAPONS AGENCY
ATTN: FCT-S, DR BALADI
ATTN: FCTO

DEPARTMENT OF THE ARMY

U S ARMY ENGR WATERWAYS EXPER STATION
ATTN: CEWES-SD-R, C WELCH
ATTN: CEWES-SE-R, D RICKMAN
ATTN: CEWES-SD-R, E JACKSON
ATTN: CEWES-SS-R, F DALLRIVA

DEPARTMENT OF THE NAVY

NAVAL RESEARCH LABORATORY
ATTN: CODE 5227 RESEARCH REPORT

DEPARTMENT OF ENERGY

LAWRENCE LIVERMORE NATIONAL LAB
ATTN: ALLEN KUHL

DEPARTMENT OF DEFENSE CONTRACTORS

APPLIED RESEARCH ASSOCIATES, INC.
ATTN: C NEEDHAM

APTEK, INC.
ATTN: B LEWIS

COLORADO UNIV AT BOULDER
2 CY ATTN: BRETT A LEWIS
2 CY ATTN: THOMAS L GEERS

GENERAL ATOMICS, INC
ATTN: CHARLES CHARMAN

H & H CONSULTANTS, INC
ATTN: W HALL

KAMAN SCIENCES CORP.
ATTN: J DRISCOLL

KAMAN SCIENCES CORPORATION
ATTN: DASIAC
ATTN: DASIAC/DARE

LOGICON R AND D ASSOCIATES
ATTN: D SIMONS
ATTN: LIBRARY

LOGICON R AND D ASSOCIATES
ATTN: G GANONG

LOGICON R AND D ASSOCIATES
ATTN: E HUMPHRIES
ATTN: J WEBSTER

MAXWELL TECHNOLOGIES INC
ATTN: T PIERCE

PACIFIC-SIERRA RESEARCH CORP.
ATTN: H BRODE

SCIENCE APPLICATIONS INTL CORP
ATTN: BILL LEE

SCIENCE APPLICATIONS INTL CORP
ATTN: D BACON

SRI INTERNATIONAL
ATTN: M SANAI

TECH REPS, INC.
ATTN: F MCMULLAN

TITAN CORPORATION (THE)
TITAN RESEARCH & TECHNOLOGY DIVSN
ATTN: R ENGLAND

TRW S. I. G.
ATTN: NORMAN LIPNER

WEIDLINGER ASSOC, INC.
ATTN: DARREN TENNANT
ATTN: H LEVINE

WEIDLINGER ASSOCIATES, INC.
ATTN: RAYMOND P DADDAZIO